PLGA microparticles entrapping chitosan-based nanoparticles for the ocular delivery of ranibizumab

Naba Elsaid [1]*, Timothy L. Jackson[2], Zeeneh Elsaid[3], Aljawharah Alqathama[3], Satyanarayana Somavarapu[3]*.
1 University of Hertfordshire, Hatfield, United Kingdom
[2] King's College London, London, United Kingdom
[3] University College London School of Pharmacy, London, United Kingdom

***Corresponding authors**
Naba Elsaid *(first)*: Email; n.elsaid@herts.ac.uk, Tele; +44(0)7783078938
Satyanarayana Somavarapu *(second)*: Email; s.somavarapu@ucl.ac.uk, Tele; +44(0)207 753 5987

Conflict of interest and financial disclosures

This study was supported by King's College Hospital NHS Foundation Trust Clinical Research and Development Investment Scheme, grant number 513843. TL Jackson received research grant support from NeoVista, Novartis, and Oraya for unrelated projects. He has served as an advisor to Alcon, Bausch & Lomb, Thrombogenics and Allimera, but received no commercial support in relation to the work presented herein.

ABSTRACT

Age-related macular degeneration (AMD) is the leading cause of certified vision loss worldwide. The standard treatment for neovascular AMD involves repeated intravitreal injections of therapeutic proteins directed against vascular endothelial growth factor, such as ranibizumab. Biodegradable polymers, such as poly(lactic-co-glycolic acid) (PLGA), form delivery vehicles which can be used to treat posterior segment eye diseases, but suffer from poor protein loading and release. This work describes a 'system-within-system', PLGA microparticles incorporating chitosan-based nanoparticles, for improved loading and sustained intravitreal delivery of ranibizumab. Chitosan-*N*-acetyl-L-cysteine (CNAC) was synthesized and its synthesis confirmed using FT-IR and ^{1}H NMR. Chitosan-based nanoparticles comprised of CNAC, CNAC/tripolyphosphate (CNAC/TPP), chitosan, chitosan/TPP (chit/TPP) or chit/TPP-hyaluronic acid (chit/TPP-HA) were incorporated in PLGA microparticles using a modified w/o/w double emulsion method. Nanoparticles and final nanoparticles-within-microparticles were characterized for their protein-nanoparticle interaction, size, zeta potential, morphology, protein loading, stability, *in vitro* release, *in vivo* anti-angiogenic activity and effects on cell viability. The prepared nanoparticles were 17 – 350 nm in size and had zeta potentials of -1.4 to +12 mV. Microscopic imaging revealed spherical nanoparticles on the surface of PLGA microparticles for preparations containing chit/TPP, CNAC and CNAC/TPP. Ranibizumab entrapment efficiency in the preparations varied between 13 – 69% and was highest for the PLGA microparticles containing CNAC nanoparticles. This preparation also showed the slowest release with no initial burst release compared to all other preparations. Incorporation of TPP to this formulation increased the rate of protein release and reduced entrapment efficiency. PLGA microparticles containing chit/TPP-HA showed the fastest and near-complete release of ranibizumab. All of the prepared empty particles showed no effect on cell viability up to a concentration of 12.5 mg/mL. Ranibizumab released from all preparations maintained its structural integrity and *in vitro* activity. The chit/TPP-HA preparation enhanced anti-angiogenic activity and may provide a potential biocompatible platform for enhanced anti-angiogenic activity in combination with ranibizumab. In conclusion, the PLGA microparticles containing CNAC nanoparticles, showed significantly improved ranibizumab loading and release profile. This novel drug delivery system may have potential for improved intravitreal delivery of therapeutic proteins, thereby reducing the frequency, risk and cost of burdensome intravitreal injections.

Keywords;
Chitosan, ranibizumab, age-related macular degeneration, sustained delivery, anti-angiogenic, hyaluronic acid

1. INTRODUCTION

Age-related macular degeneration (AMD) accounts for more UK blindness than all other eye diseases combined [1]. There are approximately 26,000 new cases of wet AMD in the UK every year [2]. Wet AMD is the most aggressive form and is usually treated with protein or aptamer-based therapy directed against vascular endothelial growth factor (VEGF); ranibizumab (Lucentis), bevacizumab (Avastin) or aflibercept (Eylea). The efficacy of these agents is limited by their short half-lives, necessitating repeated administration of expensive intravitreal injections (IVTs) [4] that are associated with rare but sight-threatening complications such as retinal detachment and endophthalmitis [5]. Further, they undergo hydrolytic breakdown by enzymes present in the vitreous and have been reported to have stability issues secondary to protein aggregation upon storage, which can potentially affect the preparation's shelf-life [6, 7]. Therefore, there is a high demand for developing a biodegradable sustained-release delivery vehicle with high protein loading and maintained protein stability. Further, the physicochemical properties, such as the size and size distribution, of the delivery vehicle influence formulation reproducibility, dose uniformity and suitability for IVT [8]. One candidate vehicle is PLGA microparticles. These are FDA approved, biodegradable drug delivery systems which have been used extensively for the controlled delivery of proteins [9, 10] and intravitreal corticosteroids like Ozurdex® (Allergan Inc., Irvine, CA, USA). However, these delivery vehicles suffer from limitations like poor protein stability, loading, an initial burst release and non-uniform particle sizes [11-13]. Studies have addressed these limitations by altering process parameters like polymer concentration, solvent composition, stabiliser concentration and the incorporation of additives [14, 15]. However, this usually overcomes only one or two limitations.

This study describes a 'system-within-system', comprised of chitosan-based nanoparticles within PLGA microparticles for intravitreal delivery of ranibizumab. Chitosan was chosen as it is a biodegradable, biocompatible polymer with potential to improve the physicochemical properties of PLGA microparticles and offers additional anti-angiogenic activity [18, 19], potentially enhancing the therapeutic effect of ranibizumab. There are many reported mechanisms for the anti-angiogenic activity of chitosan which vary with the type, molecular weight (MW) and concentration of chitosan used as well as the target cell type. It has been reported to inhibit endothelial cell migration [20] and tumour invasion [21]. Recently, chitosan has also been shown to inhibit lipopolysaccharide (LPS)-induced interleukin-8 (IL-8) production in endothelial cells involved in the pathogenesis of vascular diseases [22]. Although some studies have reported the opposite effect, namely angiogenesis [23-25].

Hyaluronic acid (HA) is a viscous polyanion which constitutes a major portion of the human vitreous humor [26] and has been used previously for sustained protein delivery [27]. What is more, as with chitosan, high molecular weight (Mw) HA has also been shown to exhibit anti-angiogenic activity [28] and has shown favourable physicochemical properties when used to coat chit/TPP nanoparticles, such as reducing size polydispersity, increasing zeta potential and improving particle size stability [29]. Given these properties, HA was assessed in this study for its effects on PLGA-based ranibizumab delivery.

A chemically-modified derivative of chitosan, chitosan-*N*-acetyl-L-cysteine (CNAC) was also used to prepare nanoparticles and compare their effects with unmodified chitosan-based nanoparticles on PLGA-based ranibizumab delivery. CNAC differs to unmodified chitosan by containing *N*-acetyl-L-cysteine (NAC) which introduces a thiol group that has been shown to form strong disulphide bonds with cysteine-rich domains of the mucus glycoproteins accounting for stronger mucoadhesive properties compared to chitosan [30]. Therefore, it may be postulated that the NAC component of CNAC forms strong disulphide bonds with the 10

cysteine residues present in ranibizumab [31] enhancing nanoparticle-protein interactions and improving loading and release of ranibizumab in PLGA microparticles. Further, VEGF has 8 cysteine residues [32], therefore, CNAC may introduce additive anti-angiogenic activity via VEGF binding and consequent neutralization. Indeed, NAC has been reported to have anti-angiogenic activity and targets multiple pathways involved in angiogenesis including oxidation and inflammation [33, 34]. Given NAC and chitosan's anti-angiogenic activity, we hypothesized that CNAC would enhance the anti-angiogenic activity of ranibizumab.

Sodium tripolyphosphate (TPP) was used as a crosslinking agent with chitosan, CNAC and chitosan/HA to form uniformly-distributed stable nanoparticles [35]. Chitosan/TPP (chit/TPP) nanoparticles have shown good ocular biocompatibility.

We aimed to develop chitosan-based nanoparticles within PLGA microparticles for improved intravitreal delivery of ranibizumab.

2. EXPERIMENTAL SECTION

2.1 Materials

The following materials were commercially obtained and used as received: hyaluronic acid sodium salt (Mw 1.5–1.8 × 10^6 Da, from *Streptococcus equi*, Fluka BioChemika, St. Louis, Mo, USA), chitosan hydrochloride (chitosan, Mw; ≤ 400 kDa, DDA 80 – 95%, Heppe Medical, Halle, Germany), PLGA (85 : 15 DL, Mw 149 kDa, Alkermes Medisorb, Wilmington Ohio, USA), ranibizumab (Novartis, Frimley, UK), Recombinant human vascular endothelial growth factor 165 (VEGF, PeproTech, NJ, USA), goat anti-human IgG F(ab')2 antibody:horseradish peroxidase (HRP, SeroTech, Oxford, UK), tetramethylbenzidine (TMB) substrate and TMB stop reagent (Surmodics/BioFX Laboratories, Eden Prairie, USA), Laemmli sample buffer (BioRad, Herts, UK), 2-mercaptoethanol (98%, Lancaster Synthesis, Lancs., UK), Coomassie Brilliant Blue stain (BioRad Laboratories, Inc., California, USA), low-growth factor synthetic matrix (Matrigel, BD Bioscience, San Jose, CA), 3-(4,5-dimethylthiazol-2-yl)-5-(3-carboxymethoxyphenyl)-2-(4-sulfophenyl)-2H-tetrazolium (MTS) and phenazine methosulfate (PMS) (CellTiter 96® AQueous One solution, Promega, Madison, WI) and mouse tumour (BD Biosciences, Bedford, UK). The following were purchased from Life Technologies (Paisley, Scotland, UK): TrypLE™ Express (1X, trypsin, EDTA, phenol red), SYTO® 9 and propidium iodide. The following materials were obtained from Fisher (Leicestershire, UK): sodium hydroxide (NaOH), glacial acetic acid, methanol, sodium chloride, sodium hydrogen carbonate, potassium chloride and potassium dihydrogen orthophosphate. The following materials were obtained from Sigma-Aldrich (St Louis, MO, USA): sodium acetate (anhydrous), polyvinyl alcohol (PVA, 87-89% hydrolysed, Mw: 13-23 kDa), *D*-(+)-trehalose dehydrate, 1-Ethyl-3-(3-Dimethylaminopropyl) carbodiimide, hydrochloride (EDAC•HCl), NAC, crystal violet (dye content ≥ 90 %), bovine serum albumin (BSA), Tween 20, cetylpyridinium chloride, sodium azide, calcium chloride, sodium tripolyphosphate, Ham's F-10 medium (pH 7.4), anhydrous dimethylsulfoxide (DMSO, > 99.9%), Dulbecco's phosphate-buffered saline (DPBS), L-glutamine 200 mM, foetal bovine serum (FBS), antibiotic-antimycotic solution (100 units/mL penicillin, 100 µg/mL streptomycin and 25 ng/mL amphotericin B), M199 medium, porcine gelatine, porcine heparin, endothelial cell growth supplement, Triton-X and sodium dodecyl sulphate (SDS) The following materials were obtained from VWR International (Lutterworth, UK): magnesium sulphate, di-sodium hydrogen phosphate dehydrate and dichloromethane (DCM, stabilised with 0.2% of ethanol). The water used throughout all of the experimental procedures was ultrapure water.

2.2 Synthesis of CNAC

CNAC was synthesised as described previously [36], with slight modifications. Briefly, 6 g of chitosan was dissolved in 100 mL of acetate buffer (pH 4.5) at room temperature. 24 g of NAC plus 8.64 g of EDAC•HCl was dissolved in 100 mL of acetate buffer under continuous stirring for 30 minutes and nitrogen atmosphere. NAC solution was then added to the chitosan solution and left to stir overnight at 4ºC under nitrogen atmosphere. This was then dialyzed (MWCO; 12-14 kDa, Medicell International, London, UK), in the dark, for 5 days and lyophilized to obtain the CNAC powder.

2.3 ^{1}H NMR and Fourier-transform-infrared (FT-IR) spectroscopy

^{1}H NMR spectra for CNAC and its native constituents (chitosan and NAC) was recorded on a Bruker 400 MHz Ultrashield NMR spectrometer (Bruker Avance, Rheinstetten, Germany). IR spectra for these components and the prepared nanoparticles were recorded on a PerkinElmer Spectrum 100 FT-IR spectrometer (spectral range of 4000 to 400 cm^{-1} PerkinElmer, Waltham, MA).

2.4 Preparation of chitosan-based nanoparticles containing ranibizumab

Chitosan-based nanoparticles containing ranibizumab were prepared to be added to PLGA microparticles (Section 2.6). The nanoparticles were composed of chitosan, chitosan/TPP (chit/TPP), chit/TPP-HA, CNAC or CNAC/TPP. 0.5% w/v chitosan or CNAC solution was prepared in 5% w/v PVA/acetate buffer (pH 5). 5 mg of ranibizumab (drug-containing nanoparticles) or an equivalent volume of water (empty particles), was added dropwise to this solution and left to stir for 15 minutes. Water (for chitosan or CNAC particles) or 0.05% w/v TPP solution (for chit/TPP, chit/TPP-HA or CNAC/TPP) was added dropwise and left to stir for a further 45 minutes. Chit/TPP-HA nanoparticles were prepared by adding 0.25% w/v of HA solution at the end. The composition of the resultant nanoparticles was chitosan (or CNAC):ranibizumab:TPP:HA in a ratio of 10:10:1:5.

2.5 Characterization of chitosan-based nanoparticles

2.5.1 Particle size and zeta potential

A Malvern Zetasizer Nano ZS (Malvern Instruments Ltd, Worcestershire, UK) instrument which utilizes dynamic light scattering (DLS) and laser Doppler velocimetry (LDV) was used to measure the size and zeta potential of the particles, respectively.

2.5.2 Morphological examination of chitosan-based particles using transmission electron microscopy (TEM)

Approximately 40 µL of the each preparation was placed on a copper grid, covered with nitrocellulose and negatively stained with 1% uranyl acetate. Images were obtained using a FEI CM 120 Bio Twin transmission electron microscope (Philips Electron Optics BV, Netherlands).

2.6 Preparation of a system-within-system, composed of chitosan-based nanoparticles-within-PLGA microparticles

Chitosan-based nanoparticles were added to PLGA microparticles using the w/o/w double emulsion method [36], with modifications. Briefly, 100 mg of PLGA was dissolved in 2.5 mL of DCM. 1 mL of primary aqueous phase containing the chitosan-based nanoparticles

(Section 2.4) was added to this and the suspension homogenised (Ultra Turrax T25 basic, Ika-Werke, Staufen, Germany) at 21 krpm for 2 minutes. The resultant primary emulsion was added to 3 mL of secondary continuous phase composed of 1% w/v PVA plus 0.5% w/v of empty chitosan-based nanoparticles, prepared as outlined in Section 2.4. To avoid creating a concentration gradient which would act as driving force for diffusion, affecting the drug entrapment efficiency and release [37] a similar concentration of nanoparticles was used in the primary phase and continuous phase for all of the preparations. The mixture was homogenised for a further 2 minutes. Solvent extraction was carried out by mixing at room temperature for 3 hours. The resultant particles were washed by centrifugation (Optima L-90K Ultracentrifuge, Beckman Coulter, Fullerton, CA) at 4°C, 21 krpm for 25 minutes. The supernatants from these washes were used to quantify the free ranibizumab content.

2.7 Characterization of nanoparticle-within-microparticle drug delivery system

2.7.1 Particle size and zeta potential

Particles were measured for their size using laser diffraction (Malvern Mastersizer S long bench, Malvern, UK) and zeta potential using LDV as outlined in Section 2.5.1.

2.7.2 Scanning electron microscopy (SEM)

Approximately 2 mg of lyophilized sample was placed onto a metal stub and sputter coated with 20 nm of gold using a Quorum Q150 (Quorum Ltd, UK). This was viewed using a scanning electron microscope (FEI Quanta 200F, Eindhoven, The Netherlands).

2.8 Determination of ranibizumab entrapment efficiency

The ranibizumab entrapment efficiency was calculated by measuring the difference between the amount of protein added and the free protein in the supernatant of the preparation, as outlined previously [38, 39]. Indirect ELISA was used for the quantification of ranibizumab. Briefly, high-binding 96-well plates (Greiner Microlon High Binding, Greiner Bio-One, Frickenhausen, Germany) were coated with 1 µg/mL of VEGF and incubated overnight at 4°C. The plates were then washed twice with PBS and blocked with 1% w/v BSA and then washed a further two times with 5% Tween 20/PBS, after which, the ranibizumab standards and samples were added. The plates were then incubated for 2 h at 37°C and washed again with 5% w/v Tween 20/PBS. This was followed by the addition of 1:4000 HRP detection antibody and incubation for 1 h at 37°C. The wash step was repeated followed by the addition of TMB substrate plus a 30 min incubation. The reaction was stopped using the stop reagent and the absorbance read at 450 nm using a microplate ultra-violet spectrophotometer (Synergy HT, Bio-Tek Instruments, VT, USA).

2.9 In vitro ranibizumab release studies

Ranibizumab released from the prepared particles was determined using the separation technique [40], by suspending the PLGA pellet in 10 mL of release medium containing Hanks' balanced salt solution (HBSS), pH 7.4 and 0.05% w/v sodium azide. This buffer was prepared as described previously [41]. The suspension was placed in air-tight containers and incubated at 37 °C with mild continuous agitation (80 rpm, orbital incubator, Gallenkamp; Loughborough, UK). At predetermined time intervals (ranging from 30 mins up to 7 months), the pH was measured to ensure minimal changes and the suspension centrifuged at 13 krpm for 15 mins. The supernatant containing the released ranibizumab was collected and

quantified using ELISA (Section 2.8). The pellet was re-suspended in fresh release medium and re-incubated. The average cumulative ranibizumab released was plotted against time.

2.10 Analysis of the structural integrity of ranibizumab released from PLGA microparticles

The structural integrity of ranibizumab released from PLGA microparticles was analysed using SDS-PAGE, as previously described [42], with modifications. Equivalent amounts of native and released ranibizumab (quantified using a BCA kit, Micro BCA Protein Assay, Pierce, Rockford, IL) were treated with sample buffer containing 2-mercaptoethanol and Laemmli buffer for 5 mins at 95 °C. The samples were then loaded onto polyacrylamide gels (Any Kd™) along with Precision Plus protein standard (both from BioRad, Herts, UK). Electrophoresis was performed at a constant voltage of 150 V for 45 mins (Bio-Rad power PAC 1000, Melville, NY). Protein bands were stained using Coomassie Brilliant Blue stain for analysis.

2.11 Cell studies

The safety of the nanoparticles-within-microparticles was assessed by analyzing their effect on mitochondrial activity via MTS assay and for any changes in cell morphology using the Live/Dead assay. Human retinal pigment epithelial (ARPE-19, American Type Culture Collection, VA, USA) cells and human vascular endothelial cells (HUVECs, Caltag Medsystems, Buckingham, UK) lines were used in this study. ARPE-19 cells were cultured in Ham's F-10 medium (pH 7.4), supplemented with 2 mM glutamine, antibiotic-antimycotic solution and 10% heat-inactivated fetal bovine serum (FBS). HUVECs were grown on cell culture flasks pre-coated with 0.1% porcine gelatin and maintained in M199 medium (pH 7.4) supplemented with 20% FBS, 2 mM L-glutamine, 100 µg/ml porcine heparin, 50 µg/ml endothelial cell growth supplement and antibiotic-antimycotic solution. The culturing medium for both HUVEC and ARPE-19 cells is referred to as complete growth medium (CGM). Both cell lines were cultured in a humidified chamber set at 37°C and 5% CO_2 atmosphere.

2.11.1 In vitro cytotoxicity studies

The effect of native ranibizumab and empty PLGA microparticles on the viability of ARPE-19 and HUVECs was determined using CellTiter 96® AQueous One solution (MTS) assay. A qualitative analysis of this effect was also carried out using fluorescence microscopy (Live/Dead assay) to investigate the effects, if any, of the samples on the morphology of the cells. 96-well plates were seeded with 2 x 10^4 cells/mL using CGM and incubated for 48 h before being replaced with low-serum (2% FBS) media and incubated for a further 12 h. Native ranibizumab (7.63 x10^5 - 2.5 mg/mL) and empty PLGA microparticles (3.81 x 10^4 - 12.5 mg/mL), together with the controls (negative: 1% Triton X and positive: untreated media) were added to the plate and incubated for a further 24 hours. Following the incubation period the MTS assay was conducted according to manufacturer's instructions, absorbance read (UV spectrophotometer, Synergy HT, Bio-Tek Instruments, VT, USA) and data normalized to untreated cells. Live/Dead assay was performed by exposing the cells to native ranibizumab and empty PLGA microparticles containing chitosan-based nanoparticles for 24 hours. A mixture of 3.34 µM SYTO® 9 and 5 µg/mL propidium iodide was then added and fluorescent images obtained (EVOS fluorescence microscope, Lifetech, UK).

2.11.2 Assessment of anti-angiogenic activity

2.11.2.1 Effect of ranibizumab released from PLGA microparticles on endothelial cell migration

Endothelial cell migration is a key process involved in angiogenesis [43]. Therefore, the anti-angiogenic activity of ranibizumab released from PLGA microparticles was assessed by analyzing inhibition of VEGF-stimulated HUVEC migration as described in [44], with modifications. HUVECs were trypsinized at 70% confluence and resuspended in low serum medium. Cells were then seeded (4 x 10^5 cells/mL) onto matrigel-coated transwell inserts (8.0 µm polycarbonate membrane, 6.5mm, Corning Costar, Cambridge, UK) and placed into lower chambers containing M199 medium supplemented with 10% FBS, 10 ng/mL VEGF (negative control) and 125 µg/mL of native ranibizumab (positive control) or ranibizumab released from PLGA microparticles. The released ranibizumab was collected as previously described [45] and concentrated to 125 µg/mL using centrifugal concentrators (10 kDa MWCO, Vivaspins, Vivascience, Hannover, Germany) which were spun at 4 krpm, 4 °C, for 15 mins (Centrifuge 5804R, Eppendorf, Germany). 125 µg/mL of ranibizumab was selected to represent the therapeutic concentration following injection into the human vitreous. The plate was then incubated for 20 h at 37°C and 5% CO_2 atmosphere. Following the incubation period, non-migrated cells were removed using a cotton swab, inserts washed twice with PBS and migrated cells fixed using absolute methanol. The migrated cells were stained using 0.5% crystal violet, viewed using a light microscope (Nikon Microphot-FXA, Nikon, Tokyo, Japan) and quantified by counting the number of cells in six random fields per insert. Images were captured using a Nikon digital camera (Nikon, Kingston upon Thames, UK) and processed using Infinity Capture application (version 6.2). Data was expressed as the percentage of cells/field (mean ± S.D, n=6) migrated in the presence of ranibizumab relative to the VEGF control.

2.11.2.2 Effect of released chitosan and chit/TPP particles with or without ranibizumab on capillary-like tubule formation

Chit/TPP-HA nanoparticles showed the highest anti-angiogenic effect and as a result was taken further to be assessed using the capillary-like tubule formation assay (V2a kit, TCS Cellworks, Buckingham, UK). Cells were exposed to VEGF (2 ng/mL) plus 125 µg/mL of native ranibizumab or ranibizumab plus chit/TPP or chit/TPP-HA nanoparticles or equivalent concentrations of empty nanoparticles. VEGF (promotes angiogenesis) and 20 µM suramin (inhibits angiogenesis) were used as the negative and positive controls, respectively. Wells were viewed using a Leitz Diavert phase contrast microscope and images captured using a Nikon digital camera (Nikon, Kingston upon Thames, UK). The images were then processed using Infinity Capture application (v. 6.2, Lumenera Corp., Canada) and tubules quantified using AngioSys 2.0 software (v. 1.0.0.2, TCS Cellworks, Buckingham, UK) for their length as previously described [46, 47]. Data was presented as the total tubule length relative to the VEGF control, for each sample (mean ± S.D, n=3).

2.12 Statistical analysis

Statistical analysis was carried out on all data using two-way analysis of variance (ANOVA) and unpaired two-tailed student *t*-test. A p value of < 0.05 was taken to be significant. Data are presented as the mean ± standard deviation (SD) from 3 independent studies, unless otherwise stated.

3. RESULTS AND DISCUSSION

3.1 Confirmation of CNAC synthesis

3.1.1 Confirmation of CNAC synthesis using FTIR

Fig. 1 shows the FT-IR spectra for the synthesised CNAC polymer and its native constituents NAC and chitosan. CNAC showed an increase in the intensity of the absorption peak at 1638 (amide I band), 1520 (amide II band) and 1311 (amide III) cm^{-1} compared to native chitosan. This is ascribed to the presence of an additional amide bond from the NAC group [48], confirming the successful synthesis of CNAC.

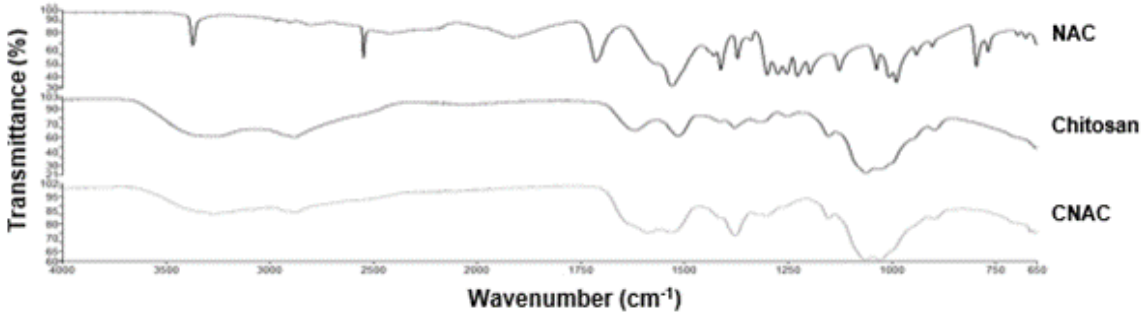

Fig. 1. FT-IR spectra for the synthesised CNAC polymer and its native constituents, chitosan and NAC. Abbreviations: NAC; N-acetyl-L-cysteine and CNAC; chitosan-N-acetyl-L-cysteine.

3.1.2 Proton nuclear magnetic resonance (^{1}H NMR)

The ^{1}H NMR spectra of CNAC (Fig. 2C) shows peaks at 2.91 and 1.97 ppm which confirm the synthesis of this polymer. The peak at 2.91 ppm corresponds to the conjugated NAC group 'CH_2SH' replacing the *N*-acetyl methyl proton seen in chitosan at 2.14 ppm (Fig. 2B). This correlates with recent findings [48]. The successful conjugation of the NAC group to chitosan was further confirmed by a peak at 1.97 ppm which was present in both NAC (Fig. 2A) and CNAC (Fig. 2C) and corresponds to the methyl proton present in both entities [49]. These findings, together with the FT-IR results, confirm the successful synthesis of the CNAC polymer.

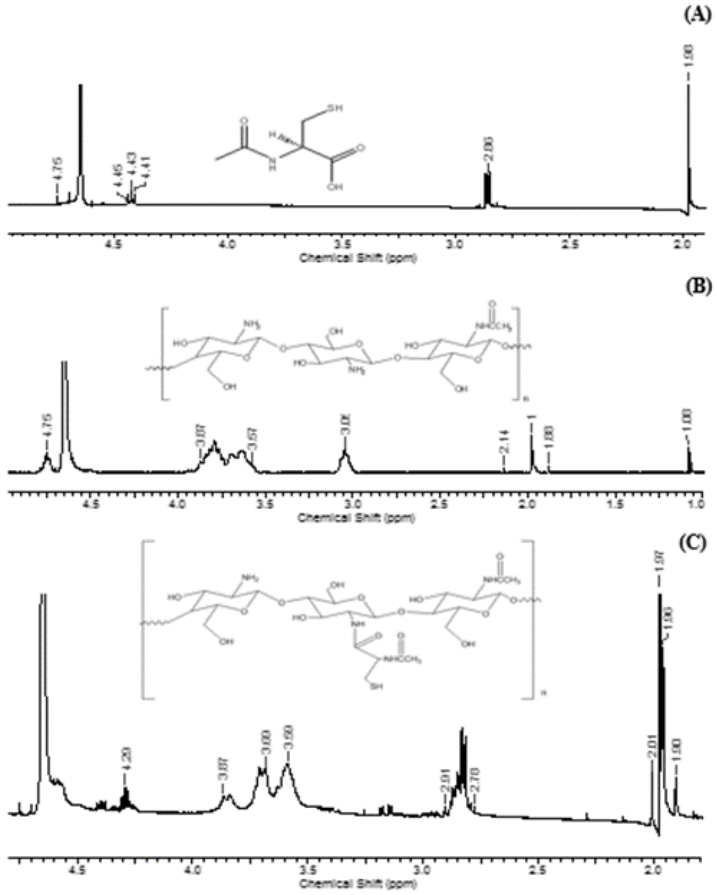

Fig. 2. ^{1}H NMR spectra of NAC (A), chitosan (B) and CNAC (C). Samples were dissolved at a concentration of 8 mg/mL in D_2O. Grey line indicates water content. Abbreviations: NAC; N-acetyl-L-cysteine and CNAC; chitosan-N-acetyl-L-cysteine.

3.2 Characterization of chitosan-based nanoparticles

Particle size, distribution, zeta potential and morphology of the nanoparticles constituting the primary aqueous phase of the preparation were analyzed as these parameters influence the stability of the primary emulsion and subsequently the protein loading and release [(50)].

3.2.1 Particle size and zeta potential

Fig 3 shows the particle size (Fig 3A) and zeta potential (Fig. 3B) of the prepared nanoparticles. The size was relatively similar to another study utilizing nanoparticles in PLGA microparticles which reported a nanoparticle size of 513 nm [(50)]. Empty chit/TPP particles were significantly larger than chitosan particles (345.5 ± 2.5 and 40.1 ± 3 nm, respectively, p = 1.79 x 10^{-8}) and previously reported chit/TPP particles of sizes up to 226 nm [(51)]. This is due to the use of a higher chitosan Mw and chit/TPP ratio of 10:1 compared 4:1 [(51)] as these parameters have been reported to influence the particle size [(52)]. Conversely, CNAC/TPP nanoparticles had a significantly smaller size of 71.8 ± 5.6 nm (p = 4.77 x 10^{-6}) compared to chit/TPP particles and previously reported CNAC/TPP nanoparticles of 166.3 nm [(48)]. Although a higher chitosan Mw was used in this study compared to Wang's study (Mw ≤ 400 kDa and 20 kDa, respectively) [(48)], the smaller particles obtained in this study may be due to the type of chitosan salt used as this has also been shown to influence the size [(52)]. This is further confirmed by comparing CNAC nanoparticles prepared from a different chitosan salt with a similar Mw to that which is used in this study; they obtained a larger size

of 214 ± 10 nm compared to 25.7 ± 2.6 nm [53]. The reason behind the significantly (p = 0.003) smaller size of CNAC nanoparticles compared to the chitosan particles was the stronger intermolecular interactions resulting from CNAC's thiol group [53, 54]. The incorporation of HA with chit/TPP did not influence the particle size significantly (chit/TPP-HA; 350.7 ± 2.5 nm) compared to chit/TPP (345.5 ± 2.5 nm; p = 0.11) but was larger than previously-reported HA chitosan nanoparticles (163 - 182 nm) [55, 56]. Native Ranibizumab had a size of 8.37 ± 0.2 nm which is in line with a previous study [57]. Entrapping ranibizumab in the chitosan-based nanoparticles had varying effects with a decrease in size obtained for chitosan and CNAC/TPP particles and an increase in size obtained for the chit/TPP-HA nanoparticles. This may be due to a difference in the interaction between the protein and the nanoparticles.

Particle zeta potential is shown in Fig. 3B. The charge of native ranibizumab was near neutral charge, at + 0.44 ± 1.5 mV and is in line with a previous study [22]. Particle zeta potential was predominantly positive as a result of the polycation, chitosan [58-60]. This decreased with the CNAC nanoparticles due to the NAC component and is in agreement with a previous study [48]. A further decrease in the positive zeta potential was observed for the chit/TPP-HA nanoparticles as a result of the polyanion, HA. However, the polyanion, TPP had different effects on the zeta potential of chitosan and CNAC nanoparticles, where there was a further decrease in the positive zeta potential of CNAC/TPP particles and no effect on the zeta potential of chit/TPP nanoparticles. This may have been due to stronger electrostatic interactions from the NAC component in CNAC with the TPP compared to the unmodified chitosan with TPP. Entrapment of ranibizumab in all of the nanoparticles caused a reduction in the zeta potential. This demonstrates ranibizumab binding to the chitosan component and is further confirmed by FT-IR (Fig. 5)

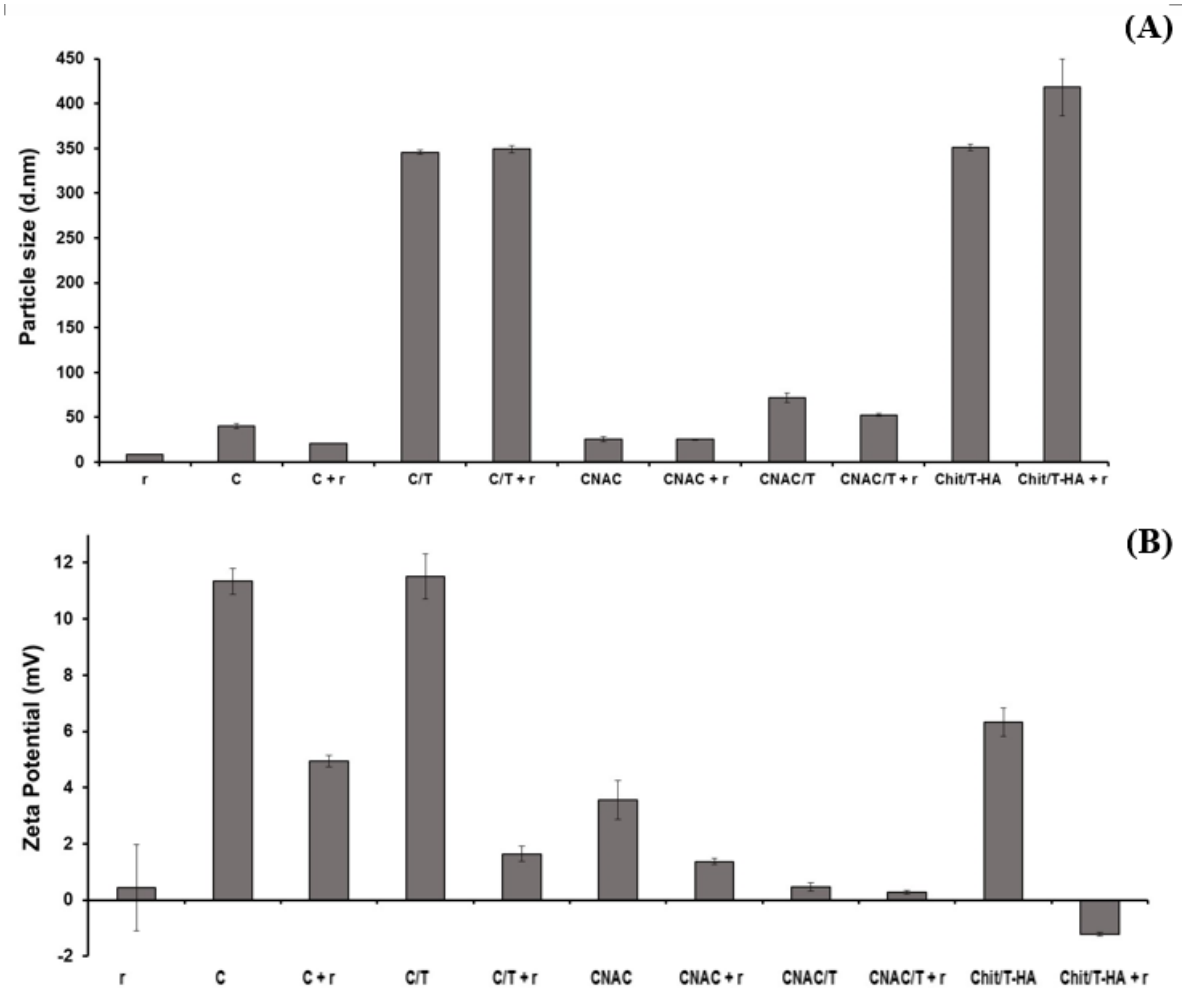

Fig. 3. Particle size (A) and zeta potential (B) of native ranibizumab and chitosan, chit/TPP, CNAC, CNAC/TPP and chit/TPP-HA with and without ranibizumab. Data are presented as the mean ± SD, n = 3. Error bars show the standard deviation. Abbreviations: r: ranibizumab, C: chitosan, C/T: chit/TPP, chit/T-HA: chit/TPP-HA, CNAC/T: CNAC/TPP, CNAC; chitosan-*N*-acetyl-L-cysteine, HA: hyaluronic acid and TPP: tripolyphosphate.

3.2.2 Nanoparticle morphology

Fig. 4 shows TEM micrographs for the chitosan-based nanoparticles containing ranibizumab. The particle sizes appeared smaller than those reported in DLS (Section 3.2.1) as TEM generates images for particles in their dry state, whereas DLS measures the particle size in their swollen state [61, 62]. However, the general trend stands, where CNAC and CNAC/TPP nanoparticles are smaller than all of the other nanoparticles. Both chitosan (Fig. 4) and CNAC (Fig. 4) nanoparticles had anisometric morphologies. TPP complexation with chitosan (Fig. $4C_x$) or CNAC (Fig. $4E_x$) caused the formation of nanoparticle islands of approximately 150 nm sizes containing smaller nanoparticles. This has been noted previously for chit/TPP nanoparticles [35, 63] but not for the CNAC/TPP nanoparticles [48] which appeared smaller compared to the chit/TPP nanoparticles (approximately 6 nm and 12-30 nm, respectively). Further inspection of the chit/TPP sample revealed novel 'globule-like' nanoparticles (Fig. $4C_{xx}$) with approximate sizes of 300 nm containing smaller nanoparticles. Chit/TPP-HA (Fig. 4D) nanoparticles appeared spherical as reported previously [56]. All of the particles were uniformly-distributed with no signs of aggregates, under TEM.

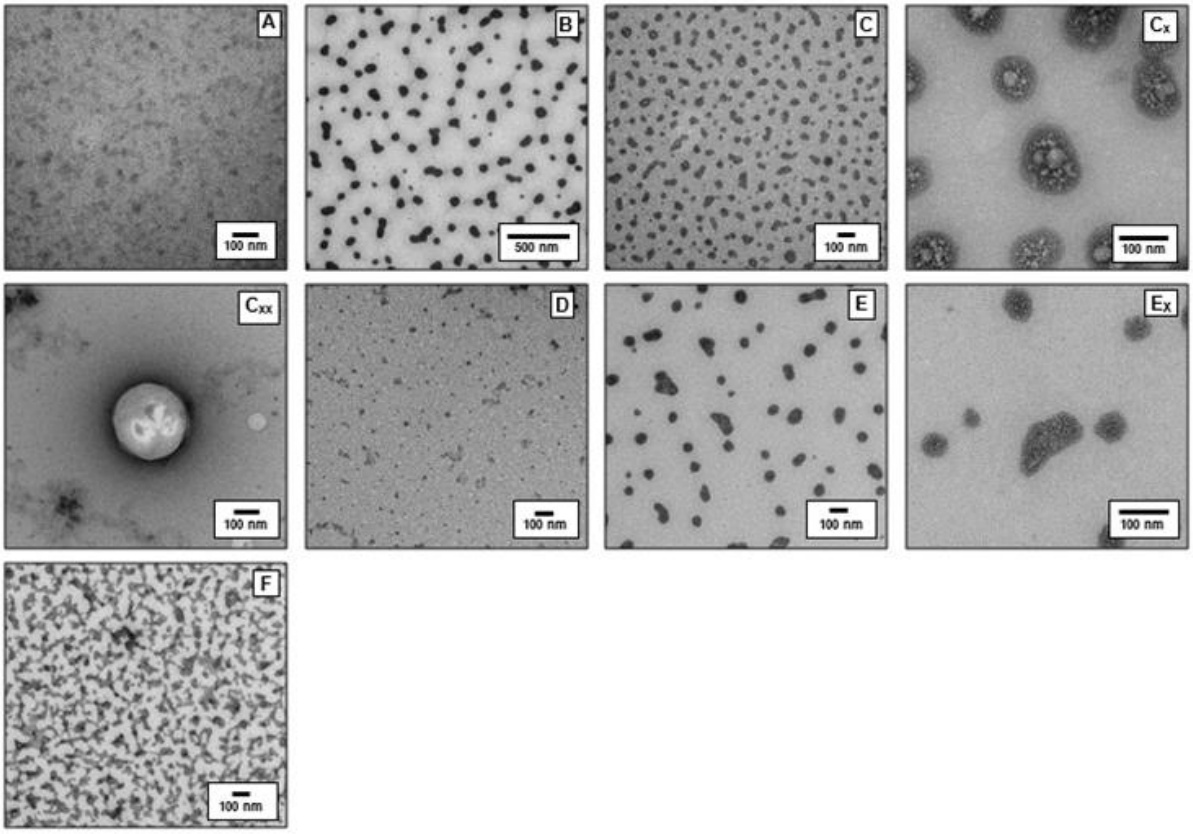

Fig. 4. TEM images of ranibizumab (A) and the following ranibizumab-containing particles: chitosan (B), chit/TPP (C, C_x, C_{xx}), chit/TPP-HA (D), CNAC (E, E_x) and CNAC/TPP (F). Abbreviations: chit/TPP; chitosan/tripolyphosphate, chit/TPP-HA; chitosan/tripolyphosphate-hyaluronic acid, CNAC; chitosan-*N*-acetyl-L-cysteine and CNAC/TPP; chitosan-*N*-acetyl-L-cysteine/tripolyphosphate.

3.2.3 Particle-protein interaction

Ranibizumab (Fig. 5A) showed absorption peaks at 995, 1037 and 1085 cm^{-1} corresponding to =C-H bending, C-F and C-O stretching, respectively [(64)]. These peaks were visible in the spectra for chitosan, chit/TPP and chit/TPP-HA (Fig. 5B), as well as CNAC and CNAC-TPP (Fig. 5C) containing ranibizumab. Thus, confirming the presence of an interaction between these particles and ranibizumab. An interaction between the P=O group of TPP and NH^{3+} present in the chitosan-based particles was apparent by the increased peak intensity at 1180 cm^{-1} [(65)]. The absorption peaks at 1625 cm^{-1} (amide I, CO stretching) and 1516 cm^{-1} (amide II, CN stretching, NH bending) of the chit/TPP-HA preparation confirms an interaction between the amino groups in chitosan and the carboxyl groups in HA [(66)].

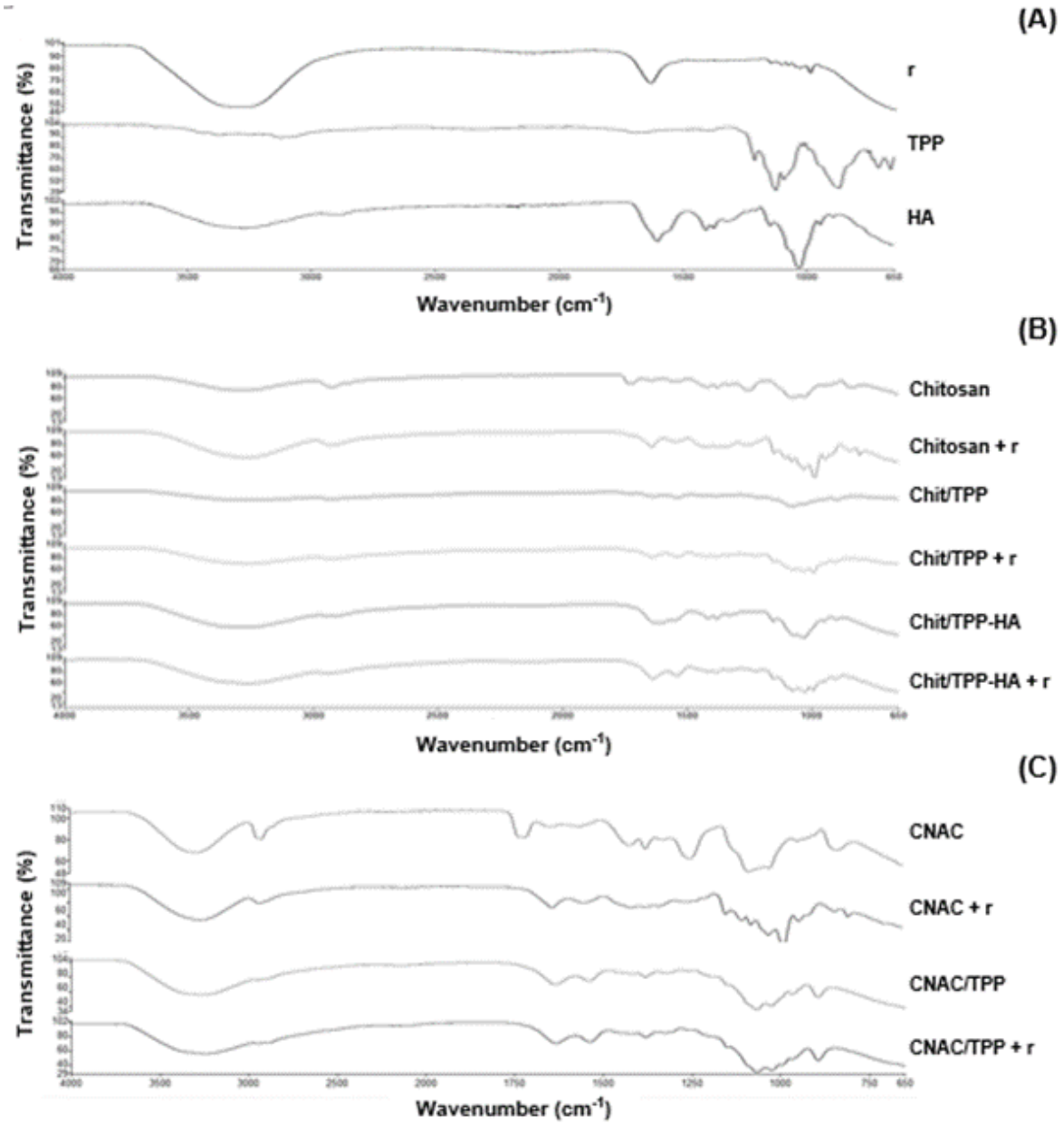

Fig. 5. FT-IR spectra for: r, TPP and HA (A), chitosan, chit/TPP and chit/TPP-HA particles with and without r (B) and CNAC and CNAC/TPP particles with and without r (C). Abbreviations: r: ranibizumab, chit/TPP; chitosan/tripolyphosphate, chit/TPP-HA; chitosan/tripolyphosphate-hyaluronic acid, CNAC; chitosan-*N*-acetyl-L-cysteine and CNAC/TPP; chitosan-*N*-acetyl-L-cysteine/tripolyphosphate.

3.3 Characterization of nanoparticle-within-microparticle drug delivery system

3.3.1 Particle size and zeta potential

The size (Fig. 6) of the nanoparticle-within-microparticle drug delivery system was measured to assess the suitability for IVT. The particle sizes were in the range of 3.04 – 6.04 µm which is considerably smaller than previously reported particles of sizes 14 – 21 µm [9, 67] which showed no effects on the retinal *in vivo* studies. Thus, based on the size, the particles appear to be suitable for IVT. The particle size distribution is also in good agreement with the SEM studies (Section 3.3.2). There was no difference in the size of the PLGA particles containing chitosan (p = 0.06), chit/TPP (p = 0.08) or chit/TPP-HA (p = 0.82) nanoparticles. However, the PLGA particles containing CNAC were significantly smaller than the control (p = 0.005) and chitosan (p = 0.0045). This is likely attributed to the NAC component which may have

increased the osmotic pressure inside the PLGA matrix, preventing inward diffusion of water molecules [68]. This may also account for the higher protein entrapment (Section 3.4) and slower release (Section 3.5). The addition of ranibizumab did not influence the size of the PLGA microparticles, with exception to those containing CNAC/TPP nanoparticles where an increase in the size was obtained relative to CNAC-containing microparticles (p = 0.0009) and the control (p = 0.004). This results from a difference in the protein-nanoparticle interaction and may account for the lower protein entrapment efficiency (Section 3.4) and higher release (Section 3.5) obtained with the CNAC/TPP preparation relative to the CNAC preparation.

Fig. 6 shows the zeta potential of the preparations. The use of chitosan increased the positive zeta potential of the overall system (- 12.2 ± 2 mV control compared to + 4.3 ± 1.6 mV, $p = 3 \times 10^{-4}$). The presence of TPP in the preparations did not influence the zeta potential of chitosan-containing preparations but reduced the positive zeta potential in CNAC/TPP compared to PLGA microparticles containing chit/TPP (p = 0.049) or CNAC (p = 0.03). This may be due to additive effect of two negatively-charged groups (TPP combined with the thiol group in CNAC).

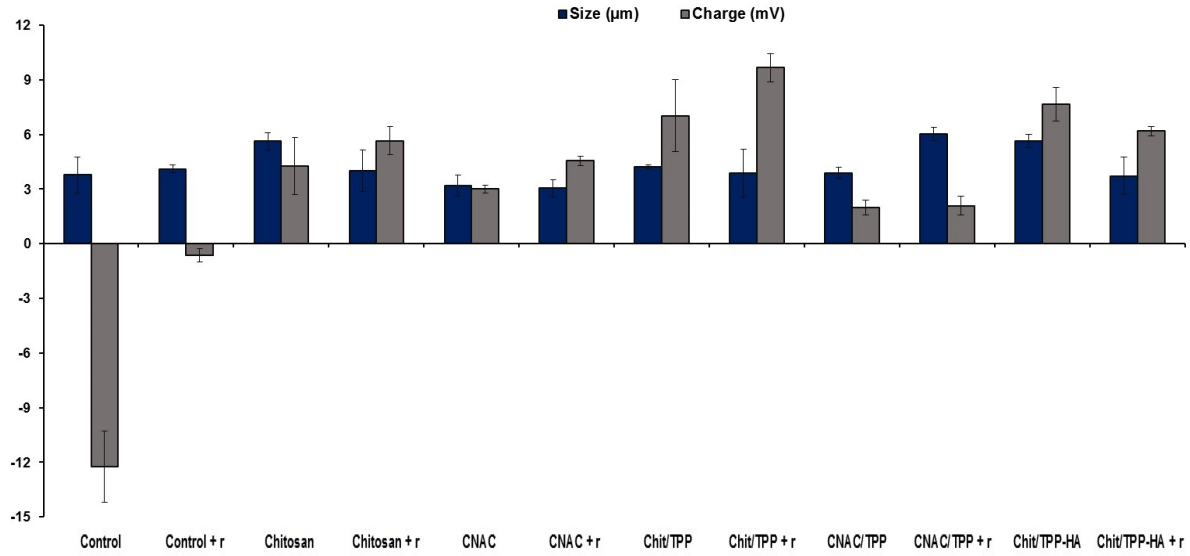

Fig. 6. Particle size (µm) and zeta potential (mV). Data are represented as the mean ± S.D., n = 3. Error bars show the standard deviation. Abbreviations: r; ranibizumab, chit/TPP; chitosan/tripolyphosphate, chit/TPP-HA; chitosan/tripolyphosphate-hyaluronic acid, NAC; *N*-acetyl-L-cysteine and CNAC; chitosan-*N*-acetyl-L-cysteine.

3.3.2 Particle morphology assessed using SEM

Fig. 7A shows the morphology of the synthesized polymer and drug delivery systems. At low magnification, the CNAC polymer has a shard-like appearance (Fig 7A). However, upon closer inspection (Fig.7 Ax), a well-defined interior of nanoparticles closely stacked together is apparent. These represent CNAC nanoparticles as it has the ability to self-assemble [53]. A difference in the particle morphology has been reported to result in different drug release profiles [69]. The PLGA control (Fig.7B) was mostly-spherical and non-uniformly-sized microparticles with an average size of 5 µm. These were smaller but had a similar surface morphology to previous findings [70]. The addition of chitosan (Fig 7C) formed a layered coat [70, 71] with the presence of rod-shaped entities (Fig. 7Cx) on the surface of the microparticles and was similar to previous findings [70].

Microparticles containing chit/TPP (Fig. 7D) had a similar morphology to these. However, the surface was coated with nanoparticles (Fig. 7Dx) of similar morphology (Fig. 7Dxx) and size distribution (DLS, Section 3.2.1) as chit/TPP nanoparticles, suggesting that these PLGA microparticles may be coated with the chit/TPP nanoparticles. A similar outcome was observed with the microparticles containing chit/TPP-HA (Fig. 7E), CNAC (Fig. 7F) and CNAC/TPP (Fig. 7G). However, the coating of the CNAC particles (Fig. 7Fx) appeared to differ in morphology to these particles and this difference may have contributed to the improved ranibizumab loading and prevention of the initial burst release. All other particles had an initial burst release with those of similar morphologies (chit/TPP, chit/TPP-HA and CNAC/TPP) having similar and higher rates of ranibizumab release relative to the control and chitosan-containing PLGA microparticles.

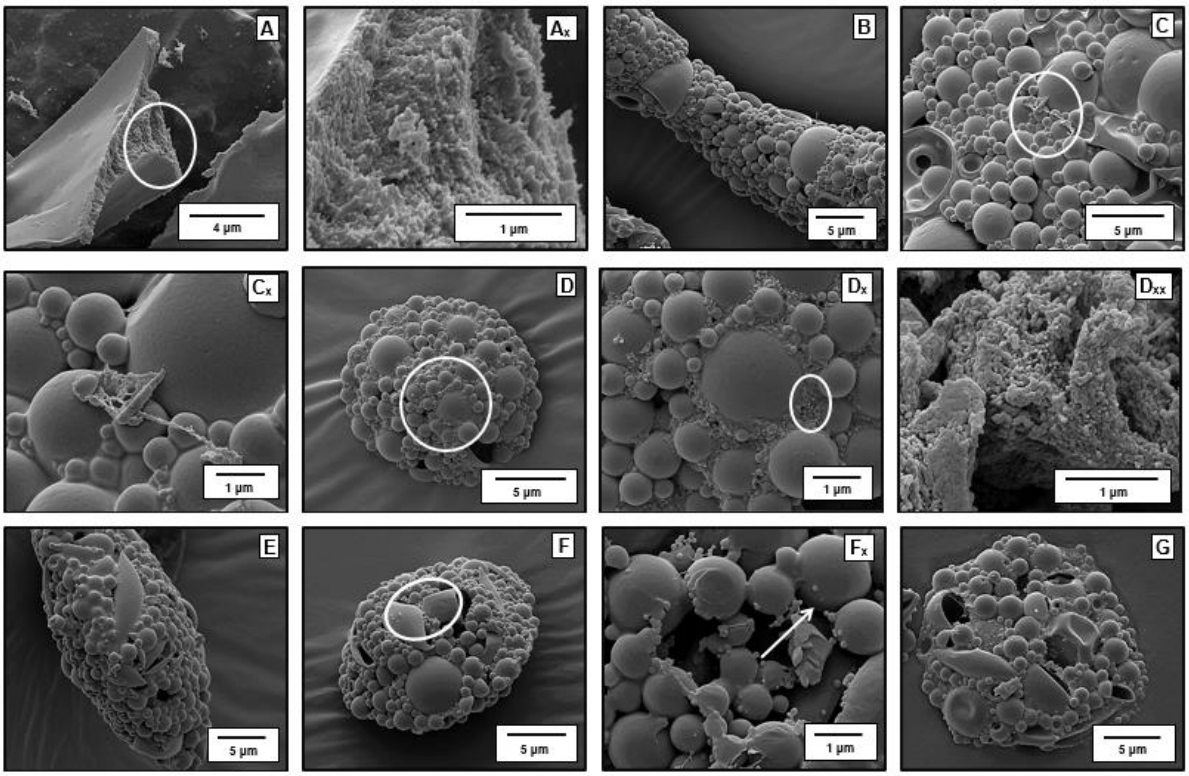

Fig. 7. Scanning electron microscopy images for CNAC polymer (A and Ax) and PLGA microparticles containing: no additions (control) (B), chitosan (C and Cx), chit/TPP (D and Dx and chitosan particles alone: Dxx), chit/TPP-HA (E), CNAC (F and Fx) and CNAC/TPP (G). Abbreviations: chit/TPP; chitosan/tripolyphosphate, chit/TPP-HA; chitosan/tripolyphosphate-hyaluronic acid, CNAC; chitosan-*N*-acetyl-L-cysteine and CNAC/TPP; chitosan-*N*-acetyl-L-cysteine/tripolyphosphate.

3.4 Ranibizumab entrapment efficiency

Fig. 8 shows the ranibizumab entrapment efficiency in the drug delivery systems. The unmodified PLGA microparticles contained 29 ± 3.8% ranibizumab which was similar to previous studies reporting an entrapment efficiency in the range of 31 - 44 % [13, 72]. The addition of chitosan nanoparticles caused a decrease ranibizumab entrapment efficiency (13 ± 2.0%, $p = 0.04$). Previous studies have shown both an increase [70] and decrease [48] in protein entrapment efficiency as a result of chitosan incorporation. This may be due to a difference in the type and Mw of chitosan used. For example, a study which used a chitosan with a much larger Mw (1000 kDa compared to ≤ 400 kDa used in this study) reported an increase in

protein entrapment [70]. The use of TPP in chit/TPP, chit/TPP-HA and CNAC/TPP did not affect the entrapment efficiency of ranibizumab relative to the control (p = 0.25, 0.89 and 0.14, respectively). Similar results were also obtained for the morphology and protein release of these particles indicating that TPP has similar interactions with the unmodified and NAC-modified form of chitosan. However, the CNAC particles had the highest ranibizumab entrapment efficiency of 69 ± 14%. This is in agreement with another study which reported improved drug loading of 62 – 76% as a result of CNAC [73]. The enhanced ranibizumab entrapment efficiency is as a result of the NAC component as this is the single entity which differentiates the particles. The reason behind this effect is yet to be elucidated, however three postulations may be put forward. First, CNAC nanoparticles increase the hydrophilicity [74] and improve ranibizumab solubilization and entrapment within the particles compared to the chitosan or chit/TPP nanoparticles [30, 53]. Second, the thiol group present in the NAC component of the CNAC nanoparticles has been reported to form strong disulphide bonds with the cysteine residues of mucus glycoproteins [30]. As ranibizumab contains 10 cysteine residues [31], it is anticipated that CNAC will form stronger interactions with ranibizumab retaining it inside the PLGA microparticles and minimizing loss during preparation. This effect may also contribute to the absence of an initial burst release and slower release compared to all of the other preparations (Section 3.5). Finally, CNAC is more viscous than chitosan [36] and studies have shown that increasing the viscosity of the PLGA matrix improves protein loading [75].

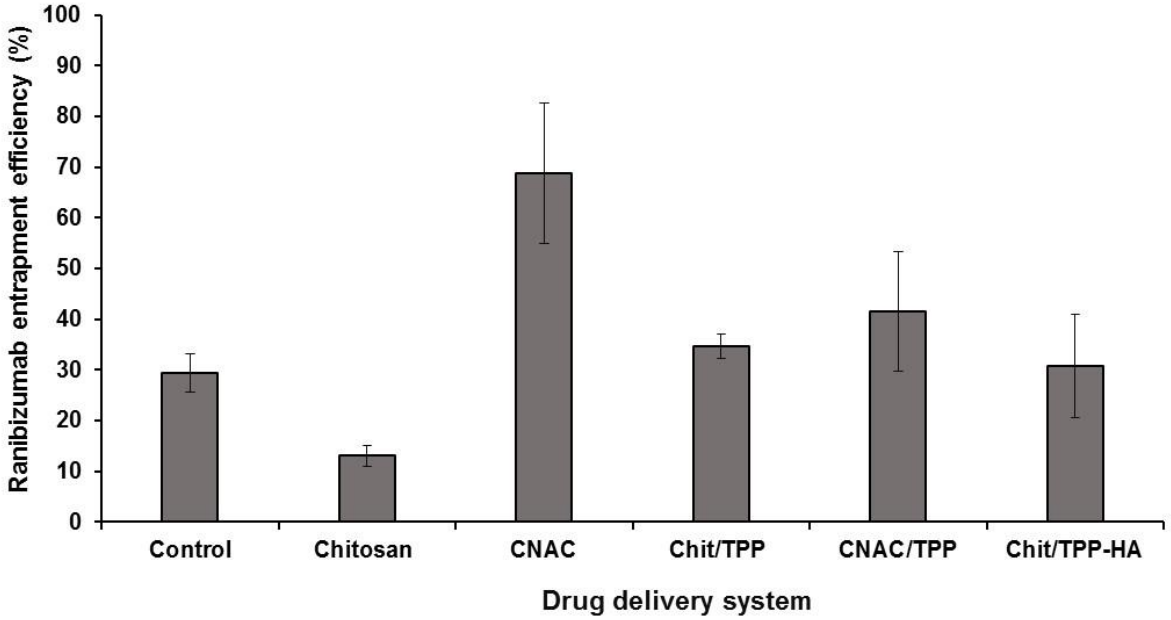

Fig. 8. Ranibizumab entrapment efficiency in PLGA (control) and PLGA microparticles containing chitosan-based particles. Data are presented as the mean ± SD, n = 3. Error bars show the standard deviation. Abbreviations: chit/TPP; chitosan/tripolyphosphate, chit/TPP-HA; chitosan/tripolyphosphate-hyaluronic acid, NAC; *N*-acetyl-L-cysteine and CNAC; chitosan-*N*-acetyl-L-cysteine.

3.5 Protein release from PLGA microparticles

The *in vitro* release of ranibizumab was investigated to determine the effect of incorporating the chitosan-based nanoparticles in the PLGA microparticles (Fig. 9). The PLGA control showed a biphasic response as previously reported [76, 77], with an initial burst release followed by a sustained-release period. The addition of chitosan did not alter the release

profile but increased the rate of protein release as reported previously [78-80]. Microparticles containing chit/TPP showed a triphasic release profile with a higher initial rate of release relative to the control. Further, chit/TPP-HA and CNAC/TPP both showed monophasic release with highest initial rate and content of release. The higher protein release obtained for chit/TPP, chit/TPP-HA and CNAC/TPP is likely attributed to the nanoparticle presentation on the microparticles and protein-nanoparticle interaction. On the other hand, PLGA microparticles containing CNAC showed a similar biphasic release profile compared to control and chitosan but was considerably lower and was the only formulation which had no initial burst release. Previous studies have also obtained release profiles for CNAC particles with no initial burst release [53, 54]. This is because CNAC has higher viscosity compared to chitosan [36] creating a viscous microenvironment which favours sustained delivery [81]. Another possible reason may be due to the presence of a thick coat, apparent in SEM (Section 3.3.2, Fig. 7Fx) as this has been reported to reduce the burst-release effect [82]. In summary, CNAC has improved the release profile of PLGA microparticles providing a potential platform for sustained intravitreal delivery of ranibizumab. PLGA microparticles containing chit/TPP-HA or CNAC/TPP may be used for the delivery of ocular drugs required for an immediate response.

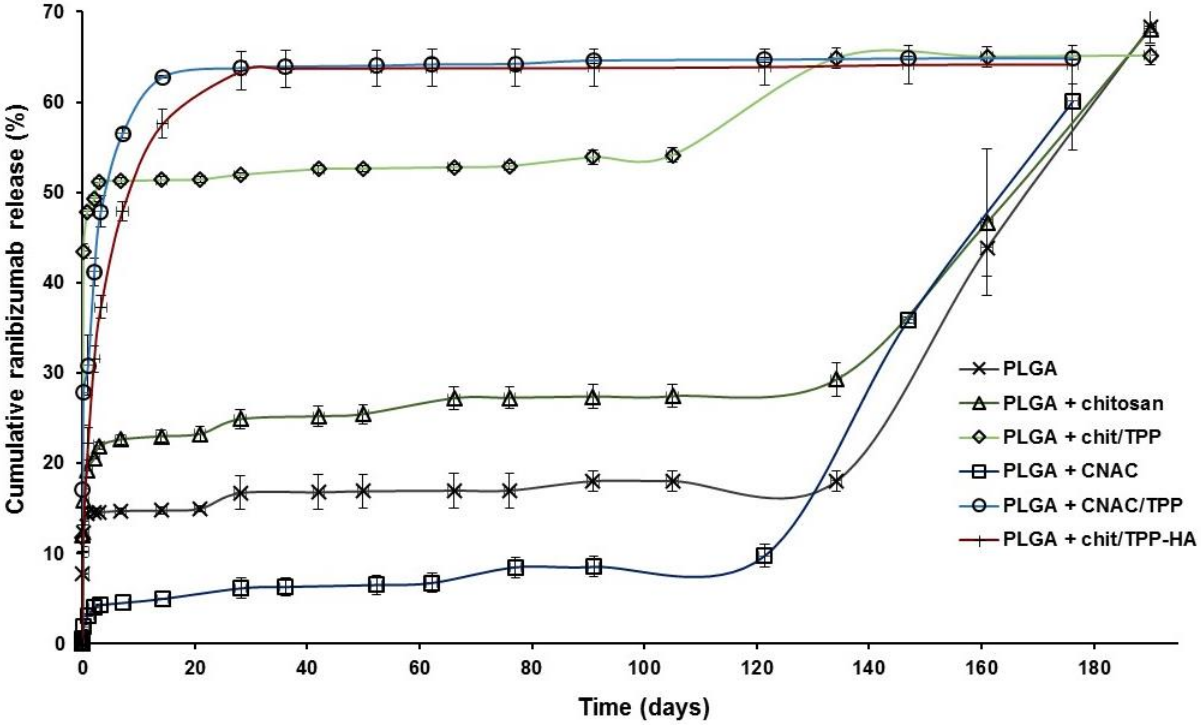

Fig. 9. Ranibizumab release from PLGA microparticles. Data are presented as the mean ± SD, n = 3. Error bars show the standard deviation. Abbreviations: chit/TPP; chitosan/tripolyphosphate, chit/TPP-HA; chitosan/tripolyphosphate-hyaluronic acid, NAC; *N*-acetyl-L-cysteine and CNAC; chitosan-*N*-acetyl-L-cysteine.

The concentration of ranibizumab which has been shown to neutralize VEGF *in vitro* is 120 ng/mL [83]. No toxic effects were obtained following exposure of ranibizumab to HUVECs and ARPE-19 cells and up to a concentration of 2.5 mg/mL in the MTS assay (Section

3.7.1.1). In the first hour, all preparations released 2.21 -35.7 µg/mL of ranibizumab and the maximum concentration released was 44.2 -207 µg/mL. Given that these values are all above 120 ng/mL (and below 2.5 mg/mL) and that ranibizumab released from all of the preparation was shown to have maintained its activity (shown by SDS-PAGE and the migration assay, Sections 3.6 and 3.7.2.1), it can be concluded that the released ranibizumab will elicit its therapeutic effect with no toxic effects.

3.6 Analysis of the structural integrity of ranibizumab released from PLGA microparticles

Fig. 10 shows the structural integrity of native ranibizumab and ranibizumab which has been released from the preparations. Native ranibizumab showed a distinctive band at 23 kDa corresponding to the reduction and cleavage of the disulfide bond between the two chains of the Fab fragment [6]. This band was also present for ranibizumab released from all of the preparations, indicating that the method of preparation and nanoparticles used did not alter the structural integrity and affect the stability of this protein. The band smearing may be a result of the high salt content from the release medium.

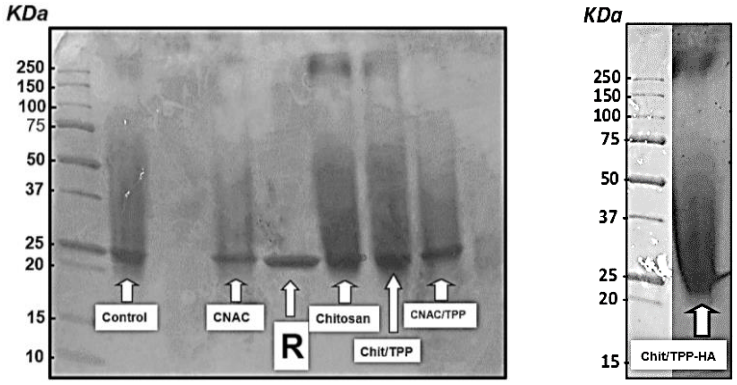

Fig. 10. SDS-PAGE band patterns for: native ranibizumab (R) and ranibizumab released from PLGA microparticles containing chitosan-based nanoparticles

3.7 Cell studies

3.7.1 Cell viability

3.7.1.1 MTS assay

Safety of ranibizumab (Fig. 11A) and the nanoparticle-within-microparticle preparations was assessed by evaluating their effects on mitochondrial activity of ARPE-19 cells (Fig. 11B) and HUVECs (Fig. 11C). A higher viability was obtained in HUVECs compared to ARPE-19 across all of the formulations and may be due to differences in cell sensitivities. Ranibizumab was well tolerated in both cell lines up to concentrations of 2.5 mg/mL (Fig. 11A), higher than the total concentration loaded in the microparticles. The biocompatibility of PLGA is well established in *in vitro* [84] and *in vivo* [85, 86] studies with reported safe concentrations of up to 25 mg/mL [87]. 12.5 mg/mL of PLGA control was used in this study and showed 80 – 109% cell viability across both cell lines. Chitosan or CNAC preparations did not significantly reduce the cell viability in both cell lines compared to control (p = 0.15 and 0.07, respectively). Chitosan has been shown to have different safety profiles, varying with the type, Mw, zeta potential of the chitosan or the cell type used [88-91]. There was also no significant difference on cell viability between CNAC and chitosan (p = (

(p = 0.95). The addition of HA did not influence the cell viability significantly (p = 0.79), as reported in recent studies [92].

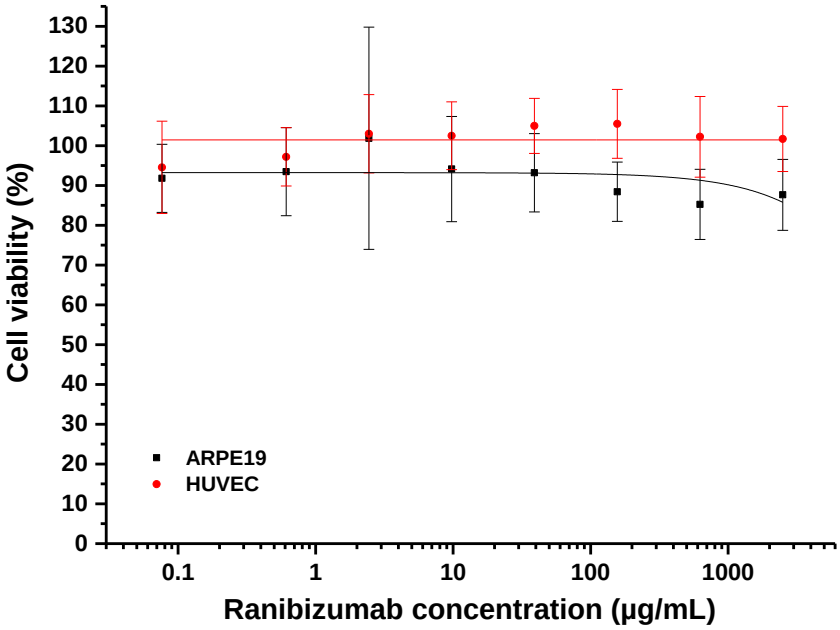

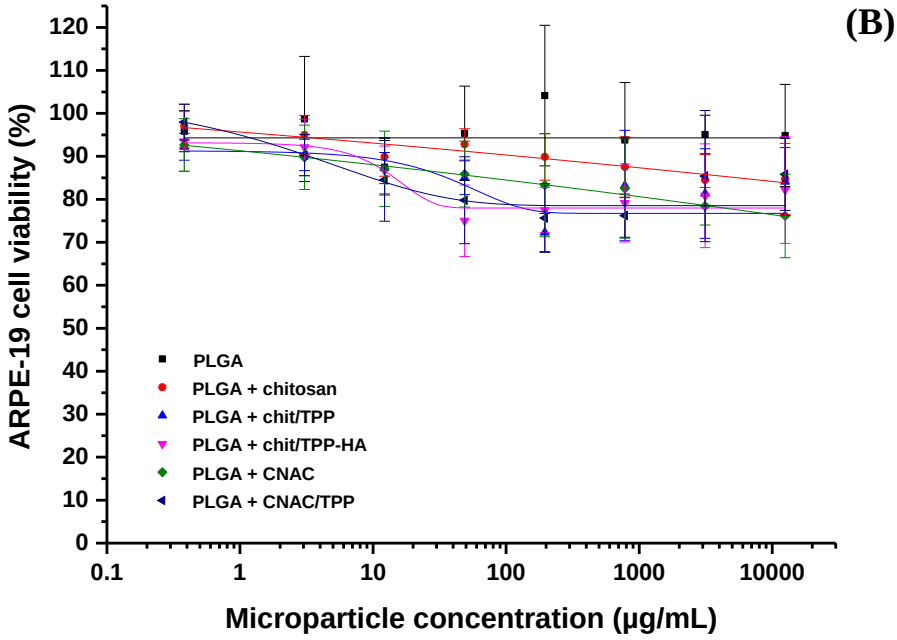

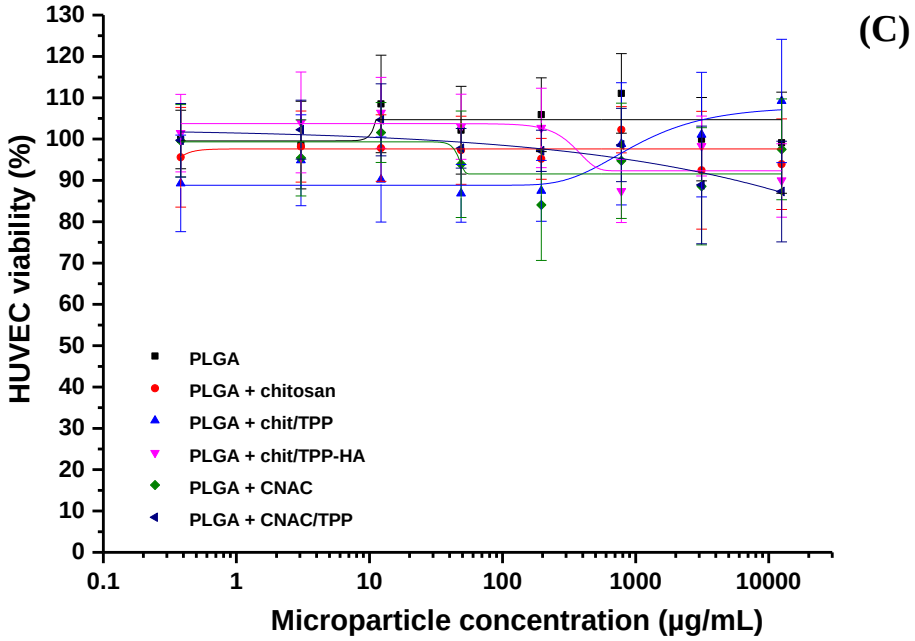

Fig. 11. Effect of ranibizumab (A) and system-within-system on the viability of ARPE-19 cells (B) and HUVECs (C). The cell viability was assessed using the MTS assay following a 24 hour exposure to ranibizumab. Data are presented as the mean ± SD, n = 9. Error bars show the standard deviation. Abbreviations: chit/TPP; chitosan/tripolyphosphate, chit/TPP-HA; chitosan/tripolyphosphate-hyaluronic acid, CNAC; chitosan-*N*-acetyl-L-cysteine and CNAC/TPP; chitosan-*N*-acetyl-L-cysteine/ tripolyphosphate. For color interpretation, the reader is referred to the online version of this article.

3.7.1.2 Live/Dead assay

The Live/Dead cell viability assay was conducted to provide a qualitative confirmation for the MTS viability assay as well as to show the effects, if any, of the drug delivery systems on the morphology of HUVECs (Fig 12A) and ARPE-19 cells (Fig 12B) [93]. Untreated ARPE-19 cells (positive controls, fluorescently-labelled green) have a cobblestone-like morphology with tight intercellular junctions [93-95]. HUVECs have a more spaced distribution with cobblestone-like appearance [96, 97]. Dead cells appear fluorescently-labelled red. The proportion of viable cells reflects the findings from the MTS assay with no morphological changes observed across the HUVECs for any of the preparations. However, ARPE-19 cells exposed cells to PLGA microparticles containing chitosan, CNAC and CNAC/TPP nanoparticles showed a more scattered appearance. This could be secondary to a loss of tight cell junctions which has been reported with chitosan as a result of induction and redistribution of cytoskeletal F-actin and tight junction protein Zona occludens (ZO-1) [98]. NAC has recently been reported to causes disassembly of the actin cytoskeleton [99] and therefore, this may also contribute to the loss of tight junctions.

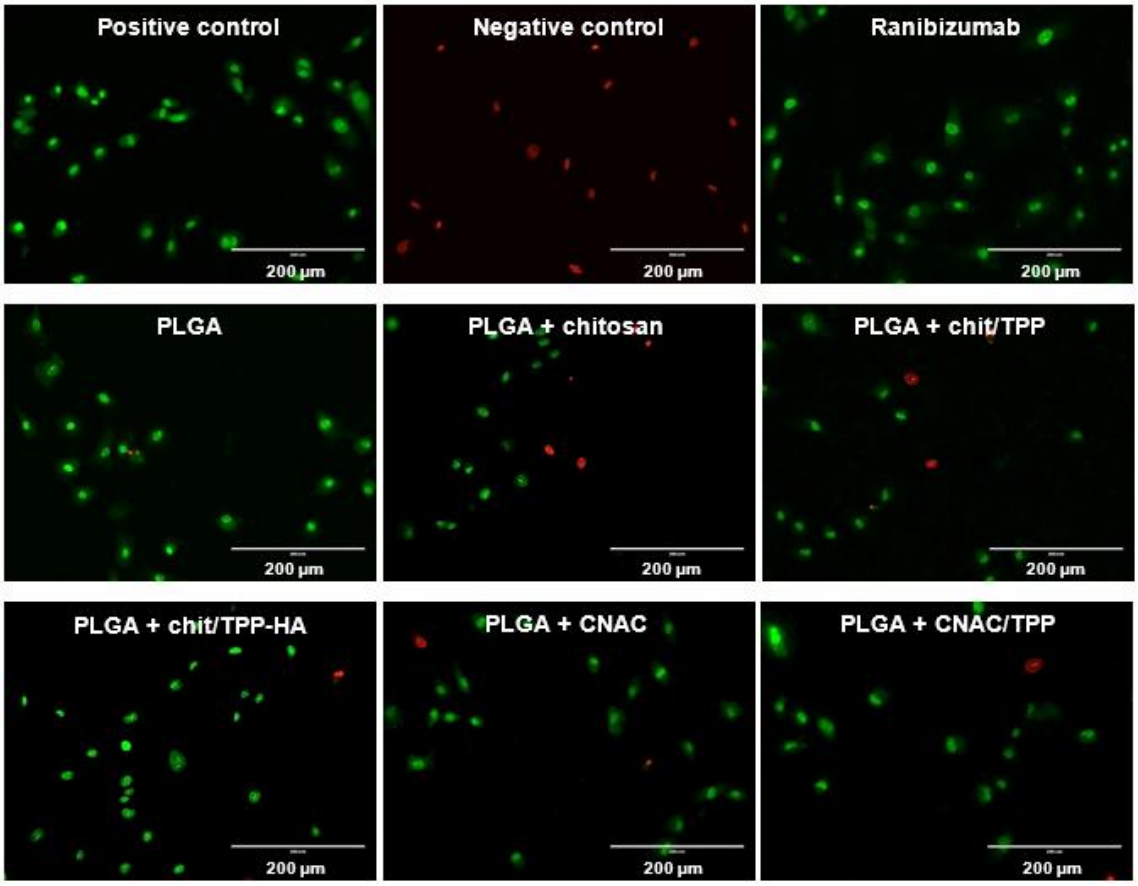

(A)

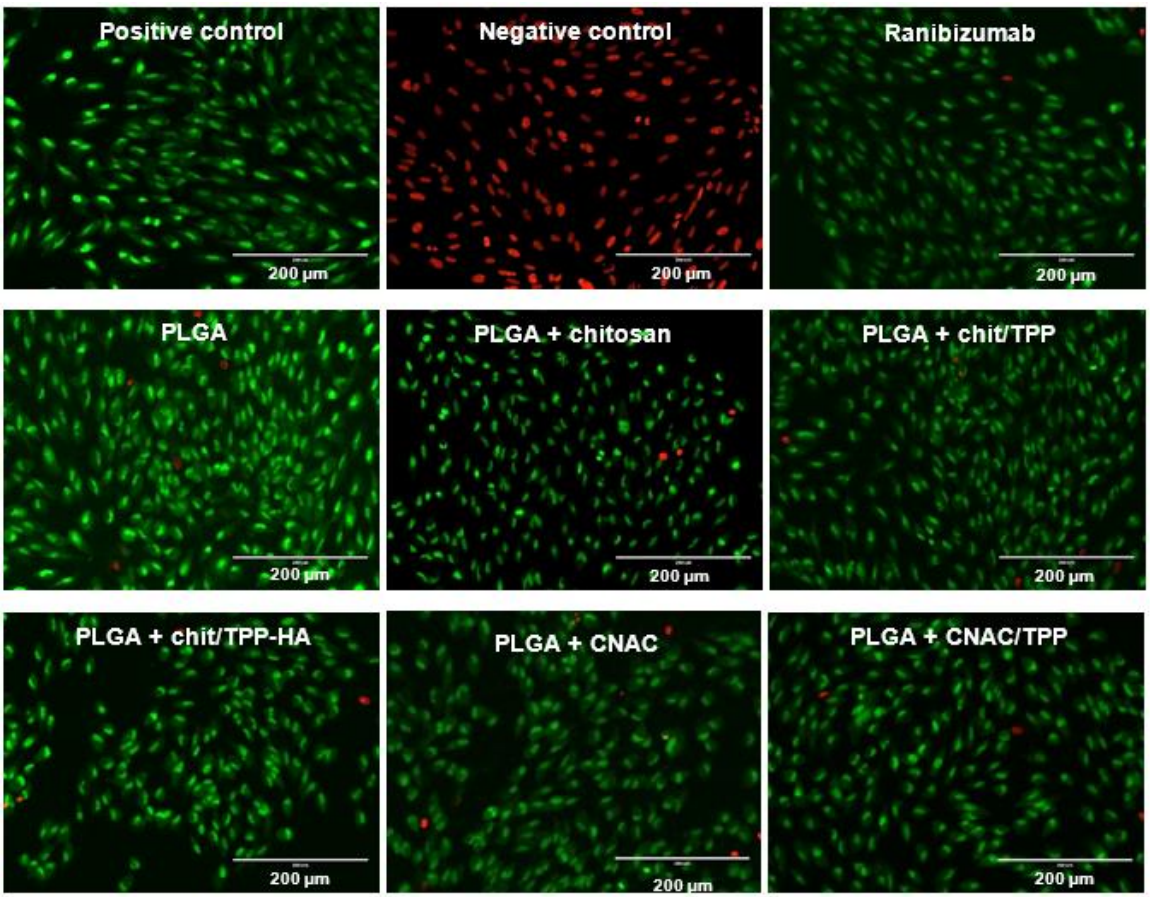

Fig. 12. Live/Dead micrographs for HUVECs (A) and ARPE-19 cells (B) exposed to 25 mg/mL of native ranibizumab and 12.5 mg/mL of empty PLGA microparticles. Green fluorescence indicates living cells, while red fluorescence indicates dead cells. Controls used were: media-treated cells (positive control) and cells treated with; 1% Triton-X (negative control). Abbreviations: chit/TPP; chitosan/tripolyphosphate, chit/TPP-HA; chitosan/tripolyphosphate- hyaluronic acid, CNAC; chitosan-*N*-acetyl-L-cysteine and CNAC/TPP; chitosan-*N*-acetyl-L-cysteine//tripolyphosphate. For color interpretation, the reader is referred to the online version of this article.

3.7.2 Assessment of anti-angiogenic activity

VEGF stimulates angiogenesis via multiple cellular pathways including endothelial cell migration [(43)], proliferation [(43)]and capillary tube formation[(43, 100)]. Ranibizumab acts by binding to VEGF and inhibiting these effects [(83, 101)]. Therefore, ranibizumab released from the preparations were analyzed for their anti-angiogenic activity using VEGF-induced cell migration and capillary-like tubule formation assays. Further, chitosan-based nanoparticles which were found to elicit an anti-angiogenic effect were further assessed using the capillary-like tubule formation assay.

3.7.2.1 Effect of ranibizumab released from PLGA microparticles on endothelial cell migration

The effect of ranibizumab, released from the prepared PLGA microparticles, on the VEGF-induced cell migration is shown in Fig. 13. A qualitative depiction of these results is shown in Fig. 14. Native ranibizumab showed an approximately five-fold decrease in VEGF-induced migration, consistent with previous reports [(102)]. Ranibizumab released from the PLGA control particles showed a similar outcome (p = 0.9) indicating that entrapment and release did not alter the activity of this protein significantly. This is in agreement with the SDS-PAGE findings (Section 3.6) showing preserved structural integrity of the released protein.

Studies utilizing PLGA for hydrophilic drug delivery have reported both maintained activity [9, 103, 104] and reduced protein stability [11, 105, 106] which result from differences in process parameters and the hydrophilic agent used. Ranibizumab released from PLGA microparticles containing CNAC and CNAC/TPP showed a slightly higher anti-migratory activity compared to ranibizumab released from control (p = 0.16 and 0.4, respectively). The NAC component may have contributed to this as it has previously been shown to inhibit VEGF-induced HUVEC tubule formation [107]. It may be postulated that this effect is secondary to disulfide interactions between the cysteine groups of NAC and VEGF[32], however, future studies should be conducted to confirm this. Further, NAC has been associated with anti-angiogenic activity in various other studies [33]. There was no significant difference between the anti-migratory effects of CNAC and CNAC/TPP (p = 0.91), suggesting that complexation of CNAC with TPP does not influence the effect caused.

Chitosan and chit/TPP nanoparticles (Fig. 13D & E, respectively) did not enhance the anti-migratory activity of ranibizumab opposing the enhanced anti-angiogenic effect obtained in the capillary-like tubule formation assay (Section 3.7.2.2). The anti-migratory activity of chitosan is not yet fully understood, with studies reporting both pro- and inhibitory effects on cell migration [23, 108, 109]. However, the difference in the anti-angiogenic activity between the two assays may be due to two reasons. First, a cell-specific effect, as the capillary-like tubule formation assay has additional human dermal fibroblasts and chitosan has been shown to inhibit tubule formation secondary to matrix metalloproteinase-2 inhibition in this cell line [21]. Another possible explanation, is that this assay considers the later stages of the angiogenic process which the migration assay does not take into account [110]. However, ranibizumab in the chit/TPP-HA-containing (Fig. 13A) preparation showed significantly higher anti-migratory activity compared to the control ($p = 6.51 \times 10^{-7}$) (Fig. 13F), which was in line with the results of the capillary-like tubule formation assay (Section 3.7.2.2). The anti-migratory effect could be associated with the HA component of the nanoparticles and is in line with a previous study [111]. Another recent study [112], showed a dose dependent inhibition, with 50% inhibition of migration with HA concentrations as low as 25 µg/mL. Although the concentration of chit/TPP-HA (or chit/TPP) nanoparticles released with ranibizumab was not quantified, the initial concentration used, assuming nothing was lost, was 625 µg/mL of this biocompatible polymer, therefore only 4% of this preparation was required to have an effect. Fig. 14 shows light micrographs of migrated HUVECs, stained with crystal violet representing a qualitative depiction of the results discussed. As Chit/TPP-HA showed the highest anti-migratory activity, it was taken forward, together with its controls (chitosan and chit/TPP), to confirm anti-angiogenic activity using a different assay i.e. capillary-like tubule formation assay.

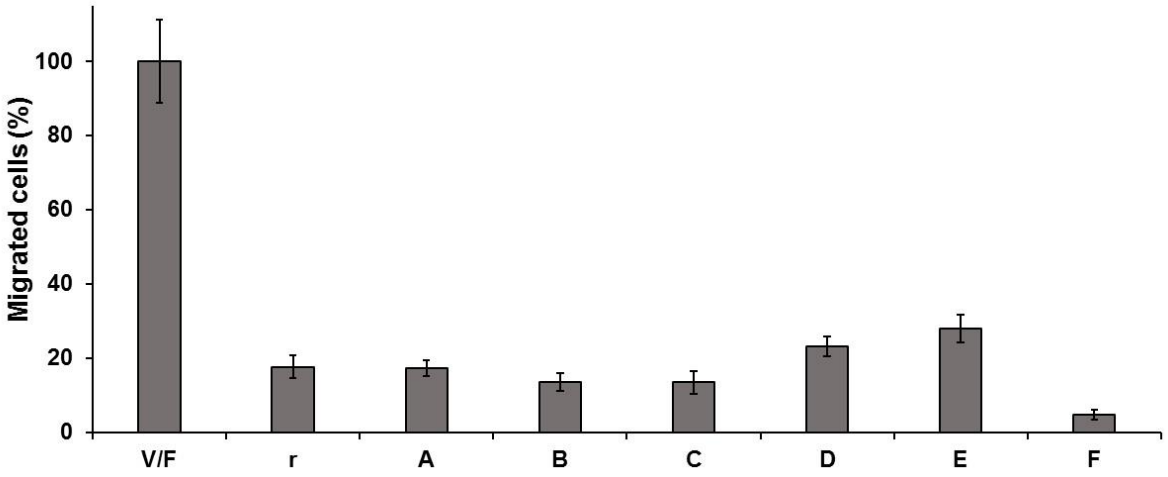

Fig. 13. HUVEC migration for cells exposed to: VEGF/FBS 10% (V/F) and VEGF/FBS 10% plus: native ranibizumab (r) or ranibizumab released from: PLGA (A), PLGA + CNAC (B) and PLGA + CNAC/TPP (C), PLGA + chitosan (D), PLGA + chit/TPP (E) or PLGA + chit/TPP-HA (F). Results are expressed as the number of cells exposed to ranibizumab per visual field (mean ± SD, n = 6) as a percentage of VEGF-stimulated migration. Error bars show the standard deviation. Abbreviations: FBS; fetal bovine serum, chit/TPP; chitosan/tripolyphosphate, chit/TPP-HA; chitosan/tripolyphosphate-hyaluronic acid, CNAC; chitosan-*N*-acetyl-L-cysteine and CNAC/TPP; chitosan-*N*-acetyl-L-cysteine/tripolyphosphate.

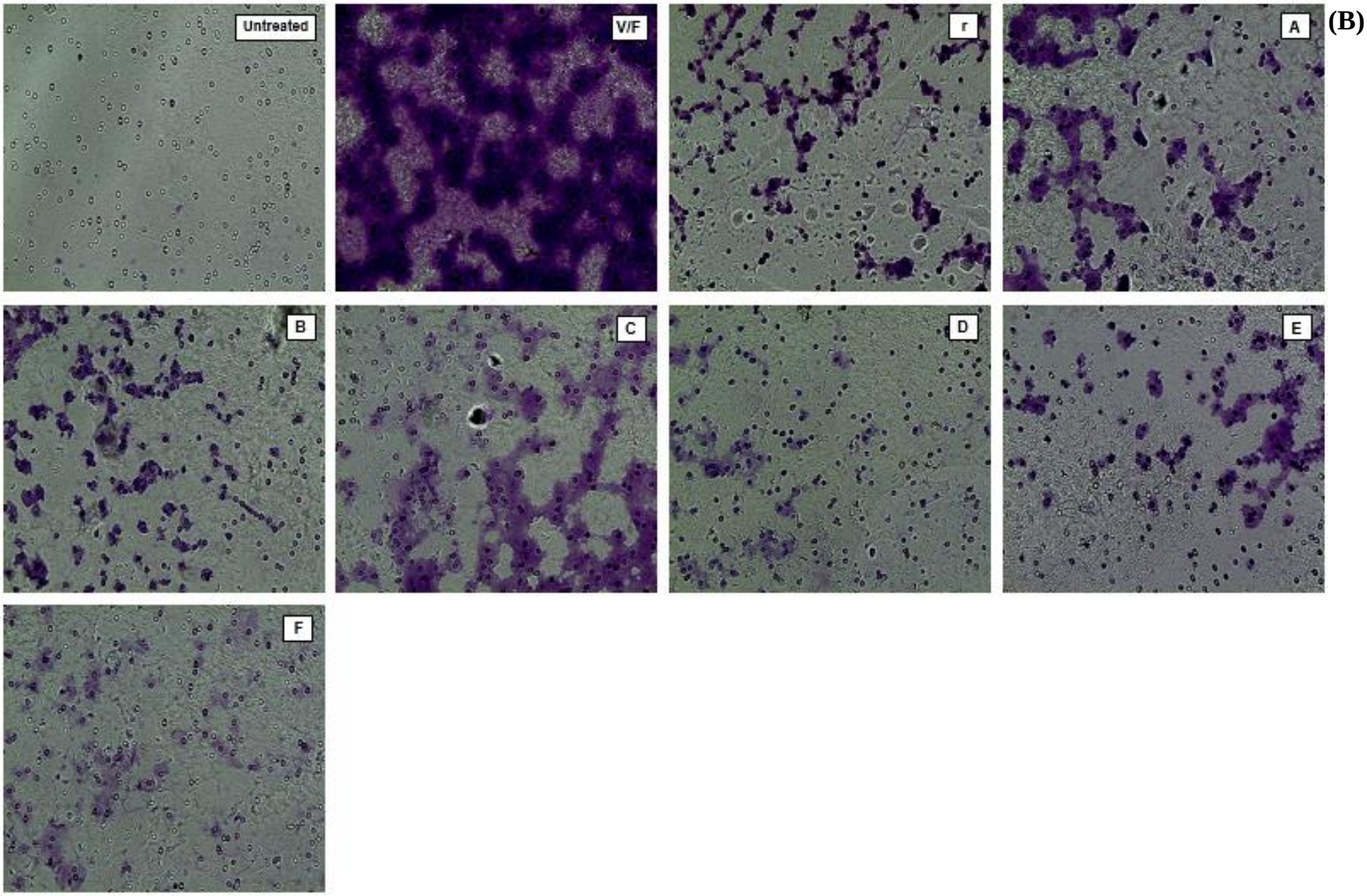

Fig. 14. Light micrographs showing migrated HUVECs for untreated cells (2% FBS) and cells exposed to: VEGF/FBS 10% (V/F), native ranibizumab (r) and ranibizumab released from: PLGA microparticles (A), PLGA + chitosan (B), PLGA + chit/TPP (C), PLGA + chit/TPP-HA (D), PLGA + CNAC (E) and PLGA + CNAC/TPP (F). Abbreviations: FBS;

fetal bovine serum, chit/TPP; chitosan/tripolyphosphate, chit/TPP-HA; chitosan/tripolyphosphate-hyaluronic acid, CNAC; chitosan-*N*-acetyl-L-cysteine and CNAC/TPP; chitosan-*N*-acetyl-L-cysteine/tripolyphosphate.

3.7.2.2 Effect of released chitosan and chit/TPP particles with or without ranibizumab on capillary-like tubule formation

Chit/TPP-HA nanoparticles showed the most significant effect in the migration study. Therefore, empty and ranibizumab-containing chit/TPP-HA and chit/TPP nanoparticles were assessed for their inhibitory effect, if any, on VEGF-induced tubule growth (Fig. 15). Suramin standard, an inhibitor of tubule growth, caused 93 ± 0.3% tubule length inhibition which was similar to a recent study, reporting 90% inhibition [113]. Native ranibizumab has been shown to cause a 50 - 70% inhibition of tubule formation at a therapeutic concentration of 125 – 200 µg/mL [102, 114, 115]. This is similar to the ranibizumab used in this study showing an inhibition of 61 ± 4.5%. Empty chit/TPP nanoparticles caused a 30 ± 1.2% inhibition, which more than doubled with the addition of ranibizumab showing a statistically significant (p = 3.73 x 10^{-3}) improvement in VEGF-mediated anti-angiogenic activity for the ranibizumab-loaded nanoparticles. The anti-angiogenic activity of chit/TPP nanoparticles may be due to their influence on VEGFR-2 levels in human dermal fibroblasts, as recently reported [19]. The empty chit/TPP-HA nanoparticles caused a higher inhibition of tubule growth relative to chit/TPP nanoparticles (p = 6.09 x 10^{-4}). This is in agreement with previous studies which have demonstrated anti-angiogenic activity following exposure to high Mw HA [28, 116]. The addition of ranibizumab to these nanoparticles demonstrated a higher inhibition relative to the chit/TPP-containing ranibizumab and native ranibizumab alone (76 ± 4.6% compared to 66 ± 3.5% and 61 ± 4.5%, respectively) and is in line with the migration assay findings.

.

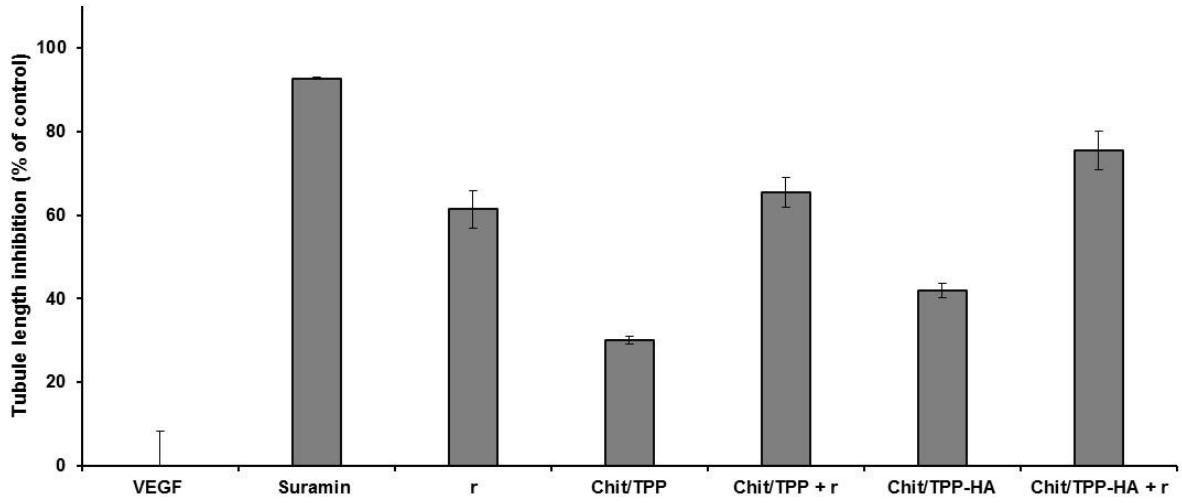

Fig. 15. Effects of empty and ranibizumab-containing chit/TPP and chit/TPP-HA nanoparticles on cell tubule length inhibition relative to VEGF-treated cells. Data are presented as the mean ± SD, n = 3. Error bars show the standard deviation. Abbreviations: r; ranibizumab, chit/TPP; chitosan/tripolyphosphate and chit/TPP-HA; chitosan/tripolyphosphate-hyaluronic acid.

4. CONCLUSION

The standard of care for the most prevalent macular diseases including wet AMD, diabetic macular oedema and retinal vein occlusion, necessitates relatively frequent IVT injections, owing to the short intravitreal half-lives of the therapeutic proteins; ranibizumab, bevacizumab and aflibercept. There is an unmet need for the development of a drug delivery system with a high entrapment efficiency and slow release of these agents. PLGA microparticles present a suitable platform for intravitreal delivery of ranibizumab as they are

biodegradable, have a safe ocular profile and have been FDA-approved for the sustained intravitreal delivery of dexamethasone (Ozurdex®). However, these microparticles are commonly associated with poor protein loading, loss of protein stability and an initial burst release, which other studies have attempted to overcome by altering the process parameters but have not succeeded in addressing all factors collectively.

Our study analysed the effects of incorporating chitosan-based nanoparticles containing ranibizumab within the PLGA microparticles on the loading, stability, activity and release of the ranibizumab, as well as their effects on the physicochemical properties of the PLGA microparticles. PLGA microparticles containing CNAC nanoparticles significantly improved ranibizumab loading, avoiding the initial burst release and a favourable prolonged release profile. These effects were perhaps related to the NAC group present in the chitosan derivative and may be as a result of the thiol interaction between the cysteine residues of NAC and ranibizumab. However, more studies are required to further investigate this. This CNAC/PLGA system-within-a-system provides a possible platform for sustained intravitreal delivery of ranibizumab, potentially reducing the frequency of IVT and the burden of care. Complexation of chitosan or CNAC with TPP increased the rate of release significantly. Therefore, these can be used to provide an immediate therapeutic effect of an intravitreal protein. Chit/TPP-HA nanoparticles showed enhanced anti-angiogenic activity (enhanced anti-migratory activity and inhibition of capillary tube formation) due to the HA component. However, PLGA microparticles containing these nanoparticles showed the fastest rate of degradation, providing a platform for immediate drug release.

Acknowledgements
We wish to thank Dr Paul Stapleton and Mr David McCarthy for their assistance in the Live/Dead, TEM and SEM procedures. We wish to also thank Robert Petrarca and Tasneem Kapadia for their contribution in the preliminary studies.

References

1. Bunce, C.; Zekite, A.; Walton, S.; Rees, A.; Patel, P.J. Certifications for sight impairment due to age related macular degeneration in England. *Public health*. **2015**,*129*,138-42.
2. NICE. Ranibizumab and pegaptanib for the treatment of age-related macular degeneration: NICE technology appraisal guidance [TA155]. 2008 [16/05/2016]. Available from: https://www.nice.org.uk/guidance/ta155/chapter/2-Clinical-need-and-practice.
3. Owen, C.G.; Jarrar, Z.; Wormald, R.; Cook, D.G.; Fletcher, A.E.; Rudnicka, A.R. The estimated prevalence and incidence of late stage age related macular degeneration in the UK. *The British journal of ophthalmology*. **2012**,*96*,752-6.
4. Bakri, S.J.; Snyder, M.R.; Reid, J.M.; Pulido, J.S.; Ezzat, M.K.; Singh, R.J. Pharmacokinetics of intravitreal ranibizumab (Lucentis). *Ophthalmology*. **2007**,*114*,2179-82.
5. Sampat, K.M.; Garg, S.J. Complications of intravitreal injections. *Current opinion in ophthalmology*. **2010**,*21*,178-83.
6. Grisanti, S.; Tura, A. [Qualitative differences between ranibizumab from original and ready to use syringes]. *Der Ophthalmologe : Zeitschrift der Deutschen Ophthalmologischen Gesellschaft*. **2010**,*107*,1123-32.
7. Kahook, M.Y.; Liu, L.; Ruzycki, P.; Mandava, N.; Carpenter, J.F.; Petrash, J.M.; Ammar, D.A. High-molecular-weight aggregates in repackaged bevacizumab. *Retina (Philadelphia, Pa)*. **2010**,*30*,887-92.

8. Ye, M.; Kim, S.; Park, K. Issues in long-term protein delivery using biodegradable microparticles. *Journal of controlled release : official journal of the Controlled Release Society*. **2010**,*146*,241-60.
9. Shelke, N.B.; Kadam, R.; Tyagi, P.; Rao, V.R.; Kompella, U.B. Intravitreal Poly(L-lactide) Microparticles Sustain Retinal and Choroidal Delivery of TG-0054, a Hydrophilic Drug Intended for Neovascular Diseases. *Drug delivery and translational research*. **2011**,*1*,76-90.
10. Yandrapu, S.K.; Upadhyay, A.K.; Petrash, J.M.; Kompella, U.B. Nanoparticles in porous microparticles prepared by supercritical infusion and pressure quench technology for sustained delivery of bevacizumab. *Molecular pharmaceutics*. **2013**,*10*,4676-86.
11. van de Weert, M.; Hennink, W.E.; Jiskoot, W. Protein instability in poly(lactic-co-glycolic acid) microparticles. *Pharmaceutical research*. **2000**,*17*,1159-67.
12. Allison, S.D. Analysis of initial burst in PLGA microparticles. *Expert opinion on drug delivery*. **2008**,*5*,615-28.
13. Hong, X.; Wei, L.; Ma, L.; Chen, Y.; Liu, Z.; Yuan, W. Novel preparation method for sustained-release PLGA microspheres using water-in-oil-in-hydrophilic-oil-in-water emulsion. *International journal of nanomedicine*. **2013**,*8*,2433-41.
14. Mao, S.; Xu, J.; Cai, C.; Germershaus, O.; Schaper, A.; Kissel, T. Effect of WOW process parameters on morphology and burst release of FITC-dextran loaded PLGA microspheres. *International journal of pharmaceutics*. **2007**,*334*,137-48.
15. Hua, F.J.; Kim, G.E.; Lee, J.D.; Son, Y.K.; Lee, D.S. Macroporous poly(L-lactide) scaffold 1. Preparation of a macroporous scaffold by liquid--liquid phase separation of a PLLA--dioxane--water system. *Journal of biomedical materials research*. **2002**,*63*,161-7.
16. Dodane, V.; Amin Khan, M.; Merwin, J.R. Effect of chitosan on epithelial permeability and structure. *International journal of pharmaceutics*. **1999**,*182*,21-32.
17. Alonso, M.J.; Sanchez, A. The potential of chitosan in ocular drug delivery. *The Journal of pharmacy and pharmacology*. **2003**,*55*,1451-63.
18. Harish Prashanth, K.V.; Tharanathan, R.N. Depolymerized products of chitosan as potent inhibitors of tumor-induced angiogenesis. *Biochimica et biophysica acta*. **2005**,*1722*,22-9.
19. Xu, Y.; Wen, Z.; Xu, Z. Chitosan nanoparticles inhibit the growth of human hepatocellular carcinoma xenografts through an antiangiogenic mechanism. *Anticancer research*. **2009**,*29*,5103-9.
20. Okamoto, H.; Umeda, S.; Obazawa, M.; Minami, M.; Noda, T.; Mizota, A.; Honda, M.; Tanaka, M.; Koyama, R.; Takagi, I.; Sakamoto, Y.; Saito, Y.; Miyake, Y.; Iwata, T. Complement factor H polymorphisms in Japanese population with age-related macular degeneration. *Molecular vision*. **2006**,*12*,156-8.
21. Kim, M.M.; Kim, S.K. Chitooligosaccharides inhibit activation and expression of matrix metalloproteinase-2 in human dermal fibroblasts. *FEBS letters*. **2006**,*580*,2661-6.
22. Liu, H.-t.; Huang, P.; Ma, P.; Liu, Q.-s.; Yu, C.; Du, Y.-g. Chitosan oligosaccharides suppress LPS-induced IL-8 expression in human umbilical vein endothelial cells through blockade of p38 and Akt protein kinases. *Acta Pharmacol Sin*. **2011**,*32*,478-86.
23. Kievit, F.M.; Cooper, A.; Jana, S.; Leung, M.C.; Wang, K.; Edmondson, D.; Wood, D.; Lee, J.S.; Ellenbogen, R.G.; Zhang, M. Aligned chitosan-polycaprolactone polyblend nanofibers promote the migration of glioblastoma cells. *Advanced healthcare materials*. **2013**,*2*,1651-9.
24. McBane, J.E.; Vulesevic, B.; Padavan, D.T.; McEwan, K.A.; Korbutt, G.S.; Suuronen, E.J. Evaluation of a collagen-chitosan hydrogel for potential use as a pro-angiogenic site for islet transplantation. *PloS one*. **2013**,*8*,e77538.

25. Miklas, J.W.; Dallabrida, S.M.; Reis, L.A.; Ismail, N.; Rupnick, M.; Radisic, M. QHREDGS enhances tube formation, metabolism and survival of endothelial cells in collagen-chitosan hydrogels. *PloS one*. **2013**,*8*,e72956.
26. Kogan, G.; Soltes, L.; Stern, R.; Gemeiner, P. Hyaluronic acid: a natural biopolymer with a broad range of biomedical and industrial applications. *Biotechnology letters*. **2007**,*29*,17-25.
27. Oh, E.J.; Park, K.; Kim, K.S.; Kim, J.; Yang, J.A.; Kong, J.H.; Lee, M.Y.; Hoffman, A.S.; Hahn, S.K. Target specific and long-acting delivery of protein, peptide, and nucleotide therapeutics using hyaluronic acid derivatives. *Journal of controlled release : official journal of the Controlled Release Society*. **2010**,*141*,2-12.
28. Rooney, P.; Kumar, S. Inverse relationship between hyaluronan and collagens in development and angiogenesis. *Differentiation; research in biological diversity*. **1993**,*54*,1-9.
29. Nasti, A.; Zaki, N.M.; de Leonardis, P.; Ungphaiboon, S.; Sansongsak, P.; Rimoli, M.G.; Tirelli, N. Chitosan/TPP and chitosan/TPP-hyaluronic acid nanoparticles: systematic optimisation of the preparative process and preliminary biological evaluation. *Pharmaceutical research*. **2009**,*26*,1918-30.
30. Bernkop-Schnurch, A.; Hornof, M.; Guggi, D. Thiolated chitosans. *European journal of pharmaceutics and biopharmaceutics : official journal of Arbeitsgemeinschaft fur Pharmazeutische Verfahrenstechnik eV*. **2004**,*57*,9-17.
31. Scientific discussion [Internet]. 2007 [cited 13.11.14].
32. Hoeben, A.; Landuyt, B.; Highley, M.S.; Wildiers, H.; Van Oosterom, A.T.; De Bruijn, E.A. Vascular endothelial growth factor and angiogenesis. *Pharmacological reviews*. **2004**,*56*,549-80.
33. Aluigi, M.G.; De Flora, S.; D'Agostini, F.; Albini, A.; Fassina, G. Antiapoptotic and antigenotoxic effects of N-acetylcysteine in human cells of endothelial origin. *Anticancer research*. **2000**,*20*,3183-7.
34. de Oliveira Dias, J.R.; Rodrigues, E.B.; Maia, M.; Magalhaes, O., Jr.; Penha, F.M.; Farah, M.E. Cytokines in neovascular age-related macular degeneration: fundamentals of targeted combination therapy. *The British journal of ophthalmology*. **2011**,*95*,1631-7.
35. Calvo, P.; Vila-Jato, J.L.; Alonso, M.a.J. Evaluation of cationic polymer-coated nanocapsules as ocular drug carriers. *International journal of pharmaceutics*. **1997**,*153*,41-50.
36. Schmitz, T.; Grabovac, V.; Palmberger, T.F.; Hoffer, M.H.; Bernkop-Schnurch, A. Synthesis and characterization of a chitosan-N-acetyl cysteine conjugate. *International journal of pharmaceutics*. **2008**,*347*,79-85.
37. Ghasemian, E.; Vatanara, A.; Rouholamini Najafabadi, A.; Rouini, M.R.; Gilani, K.; Darabi, M. Preparation, characterization and optimization of sildenafil citrate loaded PLGA nanoparticles by statistical factorial design. *Daru : journal of Faculty of Pharmacy, Tehran University of Medical Sciences*. **2013**,*21*,68.
38. Li, F.; Hurley, B.; Liu, Y.; Leonard, B.; Griffith, M. Controlled release of bevacizumab through nanospheres for extended treatment of age-related macular degeneration. *The open ophthalmology journal*. **2012**,*6*,54-8.
39. Chereddy, K.K.; Her, C.H.; Comune, M.; Moia, C.; Lopes, A.; Porporato, P.E.; Vanacker, J.; Lam, M.C.; Steinstraesser, L.; Sonveaux, P.; Zhu, H.; Ferreira, L.S.; Vandermeulen, G.; Preat, V. PLGA nanoparticles loaded with host defense peptide LL37 promote wound healing. *Journal of controlled release : official journal of the Controlled Release Society*. **2014**,*194*,138-47.
40. D'Souza, S.S.; DeLuca, P.P. Methods to assess in vitro drug release from injectable polymeric particulate systems. *Pharmaceutical research*. **2006**,*23*,460-74.

41. Liu, F.; Merchant, H.A.; Kulkarni, R.P.; Alkademi, M.; Basit, A.W. Evolution of a physiological pH 6.8 bicarbonate buffer system: application to the dissolution testing of enteric coated products. *European journal of pharmaceutics and biopharmaceutics : official journal of Arbeitsgemeinschaft fur Pharmazeutische Verfahrenstechnik eV*. **2011**,*78*,151-7.
42. Kaja, S.; Hilgenberg Jd Fau - Everett, E.; Everett E Fau - Olitsky, S.E.; Olitsky Se Fau - Gossage, J.; Gossage J Fau - Koulen, P.; Koulen, P. Effects of dilution and prolonged storage with preservative in a polyethylene container on Bevacizumab (Avastin) for topical delivery as a nasal spray in anti-hereditary hemorrhagic telangiectasia and related therapies. **2011**.
43. Folkman, J.; Klagsbrun, M. Angiogenic factors. *Science (New York, NY)*. **1987**,*235*,442-7.
44. Hotchkiss, K.A.; Ashton, A.W.; Mahmood, R.; Russell, R.G.; Sparano, J.A.; Schwartz, E.L. Inhibition of endothelial cell function in vitro and angiogenesis in vivo by docetaxel (Taxotere): association with impaired repositioning of the microtubule organizing center. *Molecular cancer therapeutics*. **2002**,*1*,1191-200.
45. Hrynyk, M.; Martins-Green, M.; Barron, A.E.; Neufeld, R.J. Sustained prolonged topical delivery of bioactive human insulin for potential treatment of cutaneous wounds. *International journal of pharmaceutics*. **2010**,*398*,146-54.
46. Iriyama, A.; Fujiki, R.; Inoue, Y.; Takahashi, H.; Tamaki, Y.; Takezawa, S.; Takeyama, K.; Jang, W.D.; Kato, S.; Yanagi, Y. A2E, a pigment of the lipofuscin of retinal pigment epithelial cells, is an endogenous ligand for retinoic acid receptor. *The Journal of biological chemistry*. **2008**,*283*,11947-53.
47. Yu, W.; Bai, Y.; Han, N.; Wang, F.; Zhao, M.; Huang, L.; Li, X. Inhibition of pathological retinal neovascularization by semaphorin 3A. *Molecular vision*. **2013**,*19*,1397-405.
48. Wang, X.; Zheng, C.; Wu, Z.; Teng, D.; Zhang, X.; Wang, Z.; Li, C. Chitosan-NAC nanoparticles as a vehicle for nasal absorption enhancement of insulin. *Journal of biomedical materials research Part B, Applied biomaterials*. **2009**,*88*,150-61.
49. Ponedel'kina, I.Y.; Odinokov, V.N.; Saitgalina, E.A.; Lukina, E.S.; Dzhemilev, U.M. Conjugation of 3′-azido-3′-deoxythymidine with heparin. *Dokl Chem*. **2008**,*419*,95-7.
50. Lee, Y.S.; Johnson, P.J.; Robbins, P.T.; Bridson, R.H. Production of nanoparticles-in-microparticles by a double emulsion method: A comprehensive study. *European journal of pharmaceutics and biopharmaceutics : official journal of Arbeitsgemeinschaft fur Pharmazeutische Verfahrenstechnik eV*. **2013**,*83*,168-73.
51. Wadhwa, S.; Paliwal, R.; Paliwal, S.R.; Vyas, S.P. Hyaluronic acid modified chitosan nanoparticles for effective management of glaucoma: development, characterization, and evaluation. *Journal of Drug Targeting*. **2010**,*18*,292-302.
52. Luangtana-anan, M.; Opanasopit, P.; Ngawhirunpat, T.; Nunthanid, J.; Sriamornsak, P.; Limmatvapirat, S.; Lim, L.Y. Effect of chitosan salts and molecular weight on a nanoparticulate carrier for therapeutic protein. *Pharmaceutical development and technology*. **2005**,*10*,189-96.
53. Talaei, F.; Azizi, E.; Dinarvand, R.; Atyabi, F. Thiolated chitosan nanoparticles as a delivery system for antisense therapy: evaluation against EGFR in T47D breast cancer cells. *International journal of nanomedicine*. **2011**,*6*,1963-75.
54. Hombach, J.; Hoyer, H.; Bernkop-Schnurch, A. Thiolated chitosans: development and in vitro evaluation of an oral tobramycin sulphate delivery system. *European journal of pharmaceutical sciences : official journal of the European Federation for Pharmaceutical Sciences*. **2008**,*33*,1-8.

55. Parajo, Y.; D'Angelo, I.; Welle, A.; Garcia-Fuentes, M.; Alonso, M.J. Hyaluronic acid/Chitosan nanoparticles as delivery vehicles for VEGF and PDGF-BB. *Drug delivery*. **2010**,*17*,596-604.
56. de la Fuente, M.; Seijo, B.; Alonso, M.J. Novel hyaluronic acid-chitosan nanoparticles for ocular gene therapy. *Investigative ophthalmology & visual science*. **2008**,*49*,2016-24.
57. Wen, H.; Hao, J.; Li, S.K. Characterization of human sclera barrier properties for transscleral delivery of bevacizumab and ranibizumab. *Journal of pharmaceutical sciences*. **2013**,*102*,892-903.
58. Janes, K.A.; Calvo, P.; Alonso, M.J. Polysaccharide colloidal particles as delivery systems for macromolecules. *Advanced drug delivery reviews*. **2001**,*47*,83-97.
59. Pan, Y.; Li, Y.J.; Zhao, H.Y.; Zheng, J.M.; Xu, H.; Wei, G.; Hao, J.S.; Cui, F.D. Bioadhesive polysaccharide in protein delivery system: chitosan nanoparticles improve the intestinal absorption of insulin in vivo. *International journal of pharmaceutics*. **2002**,*249*,139-47.
60. Qi, L.; Xu, Z.; Jiang, X.; Hu, C.; Zou, X. Preparation and antibacterial activity of chitosan nanoparticles. *Carbohydrate research*. **2004**,*339*,2693-700.
61. Aktaş, Y.; Andrieux, K.; Alonso, M.J.; Calvo, P.; Gürsoy, R.N.; Couvreur, P.; Çapan, Y. Preparation and in vitro evaluation of chitosan nanoparticles containing a caspase inhibitor. *International journal of pharmaceutics*. **2005**,*298*,378-83.
62. Ferlay, J.; Parkin, D.M.; Steliarova-Foucher, E. Estimates of cancer incidence and mortality in Europe in 2008. *European journal of cancer*. **2010**,*46*,765-81.
63. Mohammadpour Dounighi, N.; Eskandari, R.; Avadi, M.; Zolfagharian, H.; Mir Mohammad Sadeghi, A.; Rezayat, M. Preparation and in vitro characterization of chitosan nanoparticles containing Mesobuthus eupeus scorpion venom as an antigen delivery system. *J Venom Anim Toxins incl Trop Dis*. **2012**,*18*,44-52.
64. Silverstein, R.M.; Bassler, G.C.; Morrill, T.C. Spectrometric Identification of Organic Compounds; John Wiley and Sons: New York, 1981.
65. Mi, F.-L.; Shyu, S.-S.; Wong, T.-B.; Jang, S.-F.; Lee, S.-T.; Lu, K.-T. Chitosan–polyelectrolyte complexation for the preparation of gel beads and controlled release of anticancer drug. II. Effect of pH-dependent ionic crosslinking or interpolymer complex using tripolyphosphate or polyphosphate as reagent. *Journal of Applied Polymer Science*. **1999**,*74*,1093-107.
66. Yang, M.-H.; Jong, S.-B.; Lu, C.-Y.; Lin, Y.-F.; Chiang, P.-W.; Tyan, Y.-C.; Chung, T.-W. Assessing the responses of cellular proteins induced by hyaluronic acid-modified surfaces utilizing a mass spectrometry-based profiling system: Over-expression of CD36, CD44, CDK9, and PP2A. *Analyst*. **2012**,*137*,4921-33.
67. Oliveira, R.C.; Messias, A.; Siqueira, R.C.; Bonini-Filho, M.A.; Haddad, A.; Damico, F.M.; Maia-Filho, A.; Crispim, P.T.; Saliba, J.B.; Ribeiro, J.A.; Scott, I.U.; Cunha-Jr, A.S.; Jorge, R. Vitreous pharmacokinetics and retinal safety of intravitreal preserved versus non-preserved triamcinolone acetonide in rabbit eyes. *Current eye research*. **2012**,*37*,55-61.
68. Murthy, R.; Khattar, H.; Singh, S. Formulation and characterization of nano lipid carrier dry powder inhaler containing ciprofloxacin hydrochloride and N-acetyl cysteine. *International Journal of Drug Delivery*. **2012**,*4*,316-25.
69. Hsieh, D.S.; Rhine, W.D.; Langer, R. Zero-order controlled-release polymer matrices for micro- and macromolecules. *Journal of pharmaceutical sciences*. **1983**,*72*,17-22.
70. Chandy, T.; Das, G.S.; Rao, G.H. 5-Fluorouracil-loaded chitosan coated polylactic acid microspheres as biodegradable drug carriers for cerebral tumours. *Journal of microencapsulation*. **2000**,*17*,625-38.

71. Dhawan, S.; Singla, A.K. Nifedipine loaded chitosan microspheres prepared by emulsification phase-separation. *Biotechnic & histochemistry : official publication of the Biological Stain Commission*. **2003**,*78*,243-54.
72. Liu, G.; Miao, X.; Fan, W.; Crawford, R.W.; Xiao, Y. Porous PLGA microspheres effectively loaded with BSA protein by electrospraying combined with phase separation in liquid nitrogen. *Journal of Biomimetics, Biomaterials and Tissue Engineering*. **2010**,*6*,1-18.
73. Lian, H.; Zhang, T.; Sun, J.; Pu, X.; Tang, Y.; Zhang, Y.; He, Z. Enhanced paracellular and transcellular paclitaxel permeation by chitosan–vitamin E succinate–N-acetyl-l-cysteine copolymer on Caco-2 cell monolayer. *J Nanopart Res*. **2014**,*16*,1-16.
74. Pieper, G.M.; Siebeneich, W. Oral administration of the antioxidant, N-acetylcysteine, abrogates diabetes-induced endothelial dysfunction. *Journal of cardiovascular pharmacology*. **1998**,*32*,101-5.
75. Sturesson, C.; Carlfors, J. Incorporation of protein in PLG-microspheres with retention of bioactivity. *Journal of controlled release : official journal of the Controlled Release Society*. **2000**,*67*,171-8.
76. Ramchandani, M.; Robinson, D. In vitro and in vivo release of ciprofloxacin from PLGA 50:50 implants. *Journal of controlled release : official journal of the Controlled Release Society*. **1998**,*54*,167-75.
77. Amann, L.C.; Gandal, M.J.; Lin, R.; Liang, Y.; Siegel, S.J. In vitro-in vivo correlations of scalable PLGA-risperidone implants for the treatment of schizophrenia. *Pharmaceutical research*. **2010**,*27*,1730-7.
78. Murugeshu, A.; Astete, C.; Leonardi, C.; Morgan, T.; Sabliov, C.M. Chitosan/PLGA particles for controlled release of alpha-tocopherol in the GI tract via oral administration. *Nanomedicine (London, England)*. **2011**,*6*,1513-28.
79. Jain, G.K.; Pathan, S.A.; Akhter, S.; Ahmad, N.; Jain, N.; Talegaonkar, S.; Khar, R.K.; Ahmad, F.J. Mechanistic study of hydrolytic erosion and drug release behaviour of PLGA nanoparticles: Influence of chitosan. *Polymer Degradation and Stability*. **2010**,*95*,2360-6.
80. Wang, Y.; Li, P.; Kong, L. Chitosan-modified PLGA nanoparticles with versatile surface for improved drug delivery. *AAPS PharmSciTech*. **2013**,*14*,585-92.
81. Lee, E.S.; Kwon, M.J.; Lee, H.; Na, K.; Kim, J.J. In vitro study of lysozyme in poly(lactide-co-glycolide) microspheres with sucrose acetate isobutyrate. *European journal of pharmaceutical sciences : official journal of the European Federation for Pharmaceutical Sciences*. **2006**,*29*,435-41.
82. Bouissou, C.; Rouse, J.J.; Price, R.; van der Walle, C.F. The influence of surfactant on PLGA microsphere glass transition and water sorption: remodeling the surface morphology to attenuate the burst release. *Pharmaceutical research*. **2006**,*23*,1295-305.
83. Klettner, A.; Roider, J. Comparison of bevacizumab, ranibizumab, and pegaptanib in vitro: efficiency and possible additional pathways. *Investigative ophthalmology & visual science*. **2008**,*49*,4523-7.
84. Shive, M.S.; Anderson, J.M. Biodegradation and biocompatibility of PLA and PLGA microspheres. *Advanced drug delivery reviews*. **1997**,*28*,5-24.
85. Semete, B.; Booysen, L.; Lemmer, Y.; Kalombo, L.; Katata, L.; Verschoor, J.; Swai, H.S. In vivo evaluation of the biodistribution and safety of PLGA nanoparticles as drug delivery systems. *Nanomedicine : nanotechnology, biology, and medicine*. **2010**,*6*,662-71.
86. Souza, M.C.; Fialho, S.L.; Souza, P.A.; Fulgencio, G.O.; Da Silva, G.R.; Silva-Cunha, A. Tacrolimus-loaded PLGA implants: in vivo release and ocular toxicity. *Current eye research*. **2014**,*39*,99-102.

87. Yang, H.; Yang, L.; Wang, L.; Diao, Y. Preparation of Aptamer-Nanomicrocapsule Using Nanoprecipitation Method. *International Journal of Advancements in Computing Technology*. **2013**,*5*.
88. Grenha, A.; Grainger, C.I.; Dailey, L.A.; Seijo, B.; Martin, G.P.; Remuñán-López, C.; Forbes, B. Chitosan nanoparticles are compatible with respiratory epithelial cells in vitro. *European Journal of Pharmaceutical Sciences*. **2007**,*31*,73-84.
89. Manca, M.-L.; Mourtas, S.; Dracopoulos, V.; Fadda, A.M.; Antimisiaris, S.G. PLGA, chitosan or chitosan-coated PLGA microparticles for alveolar delivery?: A comparative study of particle stability during nebulization. *Colloids and Surfaces B: Biointerfaces*. **2008**,*62*,220-31.
90. Zhu, X.; Su, M.; Tang, S.; Wang, L.; Liang, X.; Meng, F.; Hong, Y.; Xu, Z. Synthesis of thiolated chitosan and preparation nanoparticles with sodium alginate for ocular drug delivery. *Molecular vision*. **2012**,*18*,1973-82.
91. Qi, W.; Pei, L.; Peifeng, L.; Tao, G.; Suming, L.; Yourong, D.; Zhirong, Z. Preparation, blood coagulation and cell compatibility evaluation of chitosan-graft-polylactide copolymers. *Biomedical Materials*. **2014**,*9*,015007.
92. Kageyama, T.; Kakegawa, T.; Osaki, T.; Enomoto, J.; Ito, T.; Nittami, T.; Fukuda, J. Rapid engineering of endothelial cell-lined vascular-like structures in in situ crosslinkable hydrogels. *Biofabrication*. **2014**,*6*,025006.
93. Giebel, S.J.; Menicucci, G.; McGuire, P.G.; Das, A. Matrix metalloproteinases in early diabetic retinopathy and their role in alteration of the blood-retinal barrier. *Laboratory investigation; a journal of technical methods and pathology*. **2005**,*85*,597-607.
94. Dunn, K.C.; Aotaki-Keen, A.E.; Putkey, F.R.; Hjelmeland, L.M. ARPE-19, a human retinal pigment epithelial cell line with differentiated properties. *Experimental eye research*. **1996**,*62*,155-69.
95. Hornof, M.; Toropainen, E.; Urtti, A. Cell culture models of the ocular barriers. *European journal of pharmaceutics and biopharmaceutics : official journal of Arbeitsgemeinschaft fur Pharmazeutische Verfahrenstechnik eV*. **2005**,*60*,207-25.
96. Feng, L.; Kienitz, B.A.; Matsumoto, C.; Bruce, J.; Sisti, M.; Duong, H.; Pile-Spellman, J. Feasibility of using hyperosmolar mannitol as a liquid tumor embolization agent. *AJNR American journal of neuroradiology*. **2005**,*26*,1405-12.
97. van der Meer, A.D.; Vermeul, K.; Poot, A.A.; Feijen, J.; Vermes, I. A microfluidic wound-healing assay for quantifying endothelial cell migration, 2010.
98. Schipper, N.G.; Olsson, S.; Hoogstraate, J.A.; deBoer, A.G.; Varum, K.M.; Artursson, P. Chitosans as absorption enhancers for poorly absorbable drugs 2: mechanism of absorption enhancement. *Pharmaceutical research*. **1997**,*14*,923-9.
99. Bozhokina, E.; Vakhromova, E.; Gamaley, I.; Khaitlina, S. N-acetylcysteine increases susceptibility of HeLa cells to bacterial invasion. *Journal of cellular biochemistry*. **2013**,*114*,1568-74.
100. Folkman, J. Tumor angiogenesis. *Advances in cancer research*. **1985**,*43*,175-203.
101. Ferrara, N.; Damico, L.; Shams, N.; Lowman, H.; Kim, R. Development of ranibizumab, an anti-vascular endothelial growth factor antigen binding fragment, as therapy for neovascular age-related macular degeneration. *Retina (Philadelphia, Pa)*. **2006**,*26*,859-70.
102. Costa, R.; Carneiro, A.; Rocha, A.; Pirraco, A.; Falcao, M.; Vasques, L.; Soares, R. Bevacizumab and ranibizumab on microvascular endothelial cells: A comparative study. *Journal of cellular biochemistry*. **2009**,*108*,1410-7.
103. Carrasquillo, K.G.; Ricker, J.A.; Rigas, I.K.; Miller, J.W.; Gragoudas, E.S.; Adamis, A.P. Controlled delivery of the anti-VEGF aptamer EYE001 with poly(lactic-co-glycolic)acid microspheres. *Investigative ophthalmology & visual science*. **2003**,*44*,290-9.

104. Pan, C.K.; Durairaj, C.; Kompella, U.B.; Agwu, O.; Oliver, S.C.; Quiroz-Mercado, H.; Mandava, N.; Olson, J.L. Comparison of long-acting bevacizumab formulations in the treatment of choroidal neovascularization in a rat model. *Journal of ocular pharmacology and therapeutics : the official journal of the Association for Ocular Pharmacology and Therapeutics*. **2011**,*27*,219-24.
105. Lu, W.; Park, T.G. Protein release from poly(lactic-co-glycolic acid) microspheres: protein stability problems. *PDA journal of pharmaceutical science and technology / PDA*. **1995**,*49*,13-9.
106. Crotts, G.; Park, T.G. Protein delivery from poly(lactic-co-glycolic acid) biodegradable microspheres: release kinetics and stability issues. *Journal of microencapsulation*. **1998**,*15*,699-713.
107. Lin, M.T.; Yen, M.L.; Lin, C.Y.; Kuo, M.L. Inhibition of vascular endothelial growth factor-induced angiogenesis by resveratrol through interruption of Src-dependent vascular endothelial cadherin tyrosine phosphorylation. *Molecular pharmacology*. **2003**,*64*,1029-36.
108. Okamoto, Y.; Watanabe, M.; Miyatake, K.; Morimoto, M.; Shigemasa, Y.; Minami, S. Effects of chitin/chitosan and their oligomers/monomers on migrations of fibroblasts and vascular endothelium. *Biomaterials*. **2002**,*23*,1975-9.
109. Chen, Y.L.; Wang, C.Y.; Yang, F.Y.; Wang, B.S.; Chen, J.Y.; Lin, L.T.; Leu, J.D.; Chiu, S.J.; Chen, F.D.; Lee, Y.J.; Chen, W.R. Synergistic effects of glycated chitosan with high-intensity focused ultrasound on suppression of metastases in a syngeneic breast tumor model. *Cell Death Dis*. **2014**,*5*,e1178.
110. Arnaoutova, I.; Kleinman, H.K. In vitro angiogenesis: endothelial cell tube formation on gelled basement membrane extract. *Nature protocols*. **2010**,*5*,628-35.
111. Jin, S.G.; Jeong, Y.I.; Jung, S.; Ryu, H.H.; Jin, Y.H.; Kim, I.Y. The effect of hyaluronic Acid on the invasiveness of malignant glioma cells : comparison of invasion potential at hyaluronic Acid hydrogel and matrigel. *Journal of Korean Neurosurgical Society*. **2009**,*46*,472-8.
112. Ito, T.; Williams, J.D.; Al-Assaf, S.; Phillips, G.O.; Phillips, A.O. Hyaluronan and proximal tubular cell migration. *Kidney international*. **2004**,*65*,823-33.
113. Wang, Z.; Perez, M.; Caja, S.; Melino, G.; Johnson, T.S.; Lindfors, K.; Griffin, M. A novel extracellular role for tissue transglutaminase in matrix-bound VEGF-mediated angiogenesis. *Cell Death Dis*. **2013**,*4*,e808.
114. Carneiro, A.; Falcao, M.; Pirraco, A.; Milheiro-Oliveira, P.; Falcao-Reis, F.; Soares, R. Comparative effects of bevacizumab, ranibizumab and pegaptanib at intravitreal dose range on endothelial cells. *Experimental eye research*. **2009**,*88*,522-7.
115. Medina, R.J.; O'Neill, C.L.; Devine, A.B.; Gardiner, T.A.; Stitt, A.W. The Pleiotropic Effects of Simvastatin on Retinal Microvascular Endothelium Has Important Implications for Ischaemic Retinopathies. *PloS one*. **2008**,*3*,e2584.
116. Feinberg, R.N.; Beebe, D.C. Hyaluronate in vasculogenesis. *Science (New York, NY)*. **1983**,*220*,1177-9.
117. Kean, T.; Roth, S.; Thanou, M. Trimethylated chitosans as non-viral gene delivery vectors: cytotoxicity and transfection efficiency. *Journal of controlled release : official journal of the Controlled Release Society*. **2005**,*103*,643-53.
118. Mura, S.; Hillaireau, H.; Nicolas, J.; Le Droumaguet, B.; Gueutin, C.; Zanna, S.; Tsapis, N.; Fattal, E. Influence of surface charge on the potential toxicity of PLGA nanoparticles towards Calu-3 cells. *International journal of nanomedicine*. **2011**,*6*,2591-605.
119. Dawson, J.R.; Norbeck, K.; Anundi, I.; Moldeus, P. The effectiveness of N-acetylcysteine in isolated hepatocytes, against the toxicity of paracetamol, acrolein, and paraquat. *Archives of toxicology*. **1984**,*55*,11-5.

120. Tsai, J.C.; Jain, M.; Hsieh, C.M.; Lee, W.S.; Yoshizumi, M.; Patterson, C.; Perrella, M.A.; Cooke, C.; Wang, H.; Haber, E.; Schlegel, R.; Lee, M.E. Induction of apoptosis by pyrrolidinedithiocarbamate and N-acetylcysteine in vascular smooth muscle cells. *The Journal of biological chemistry*. **1996**,*271*,3667-70.

For Table of Contents Only